IEEE Access
Multidisciplinary : Rapid Review : Open Access Journal

Received 1 November 2023, accepted 2 December 2023, date of publication 5 December 2023,
date of current version 21 December 2023.

Digital Object Identifier 10.1109/ACCESS.2023.3340138

RESEARCH ARTICLE

Bidirectional Selective Detect-and-Forward (DetF) Multi-Relay Systems With Regularized WDFDC Receivers

JUNQIAN ZHANG[1] AND HARRY LEIB[2], (Life Senior Member, IEEE)
[1]Analog Devices Inc., Toronto, ON M5G 2C8, Canada
[2]Department of Electrical and Computer Engineering, McGill University, Montreal, QC H3A 0E9, Canada
Corresponding author: Harry Leib (harry.leib@mcgill.ca)

ABSTRACT In this work, we consider a selective Detect-and-Forward (a symbol based decode-and-forward) (DetF) multi-relay two-way network employing differential MPSK with regularized Weighted Decision Feedback Differential Coherent (WDFDC) receivers. Regularized WDFDC receivers based on a regularized linear predictor (RLP) were proposed for one-way relay networks where it was shown to mitigate the performance loss due to decision feedback error propagation and intermittent transmission between relay nodes and the destination.This paper introduces regularized WDFDC receivers for two way selective DetF relay networks, employing various protocols with and without network coding, and using multiple relays. For each protocol, an optimal destination threshold is derived to decide if a relay transmits or remains silent. Furthermore, analytical performance bounds, providing insights to the effects that cause degradation, are also derived. Extensive simulation results demonstrate that the use of network coding achieves higher bandwidth efficiency, but suffers an error rate performance loss. Diversity gains can be achieved when the number of relays increases. However, repeated transmissions from the same relay do not yield extra diversity gains.

INDEX TERMS Cooperative communication, relaying systems, differential detection, noncoherent detection, differential modulation.

I. INTRODUCTION

Interest in cooperative communications and relay networks has increased dramatically over recent years since such systems provide diversity advantages with relatively low complexity [1], [2], [3], [4], [5], [6], [7], [8], [9], [10], [11]. The Two-Way Relay Network (TWRN), where two terminals exchange information with the assistance of a relay, has received much attention in the literature [5], [6], [7], [9], [11] since it achieves higher transmission efficiency and network throughput than in One-Way Relay Network (OWRN) [12]. In particular biderectional relaying has been found of interest to 6G systems [1] and IoT applications [2]. Based on the number of phases required for the bidirectional data exchange, TWRN schemes can be classified into three main categories. With a traditional transmission scheduling scheme, the data exchange requires four phases, which is essentially OWRN applied in each of the two directions [13]. With such a scheme the spectrum is not used efficiently. Exploiting the broadcast nature of a wireless channel, the three phases protocol improves spectral efficiency by employing network coding [14]. With such a scheme a relay needs only one phase to broadcast the network-coded signal to both destinations. In [15], a three phases protocol was proposed also for Decode-and Forward (DF) relaying in multi-hop wireless networks, where the bitwise XOR operation is performed at the relay. In [16], optimal and suboptimal non-coherent detectors are proposed for three phases Amplify and Forward (AF) TWRN over fast Rayleigh fading channels. The spectral efficiency can be further improved by reducing the total transmissions to two phases, where both terminals transmit simultaneously to the

The associate editor coordinating the review of this manuscript and approving it for publication was Mohamed M. A. Moustafa.

relay in the first phase and the relay broadcasts in the second phase. However, since all nodes work in half-duplex mode, the two terminals cannot listen to each other in the first phase and therefore the direct link transmission cannot be easily exploited. It has been shown that the end-to-end performance of a relay network depends significantly on the detection reliability at relay nodes [17]. With imperfect detection, the diversity gain degrades because of error propagation. In [18], [19], and [20], selective DF is used for OWRN where the relay forwards only correctly decoded symbols, and remains silent otherwise. In [21], selective DF relaying is extended to TWRN using a three phases protocol.

In a TWRN system it is difficult for terminals and relay nodes to estimate the channel accurately, especially in fast fading environments. Hence, differential modulation is preferred since no CSI is needed with differential coherent detection. The Decision-Feedback Differential Coherent (DFDC) detector [22] constitutes a low complexity better performing technique exploiting feedback from previously decoded symbols that was originally introduced for AWGN channels and extended to fading channels in [23] and [24]. The DFDC receiver was also considered for differential quadrature amplitude modulation (DQAM) in [25]. Iterative techniques based on DFDC detection were applied in [26] to massive MIMO systems. Furthermore, the DFDC receiver has been considered also for cooperative communication systems. In [27], a DFDC detector was considered for a TWRN system employing a single-relay AF protocol. Weighted-DFDC (WDFDC) receivers were considered for selective DF one-way multi-relay networks in [20], and shown that over fast fading channels they provide significant performance gains. In [28] low complexity regularized WDFDC receivers based on a regularized linear predictor (RLP) were considered for the relay-destination channel in OWRN. It was shown that the effect of decision feedback error propagation and intermittent transmissions are reduced and the performance of OWRN is significantly improved.

This paper considers a symbol based selective DF technique termed Detect-and-Forward (DetF) bi-directional multi-relay TWRN system. This scheme uses the novel regularized WDFDC receivers of [28] and SNR-dependent thresholds at the destination. Various transmission protocols consisting of multiple relays with and without network coding are considered. For each protocol, an optimum threshold for a likelihood ratio test that maximizes $(P_d - P_f)$ is derived and applied at both destinations. Furthermore, analytical performance bounds are derived for each protocol. In [29, App. B], the error probability of multichannel binary signals is derived assuming independent channels. In this paper, we extend the analysis to correlated channels, which corresponds to protocols where the destination receives multiple signals from the same relay in one time slot. Extensive simulation results over fast fading channels are provided to illustrate the system performance. The main contributions of this paper are:

1) The introduction of a novel approach employing WDFDC receivers in two way DetF relay systems with differential encoding and hence not requiring channel state information for demodulation.

2) Consideration and comparison of seven relaying protocols for the above system, with and without network coding.

3) Performance analysis through various novel analytical bounds to probability of error, as well as extensive computer simulations.

The rest of this paper is organized as follows. Selective DetF multi-relay TWRN systems with various protocols and regularized WDFDC receivers are introduced in section II. Analytical performance bounds are derived in section III. Performance simulation results for all protocols are presented in section IV and the conclusions are drawn in section V. The appendix provides derivation details for the threshold of the likelihood ratio test employed in this system.

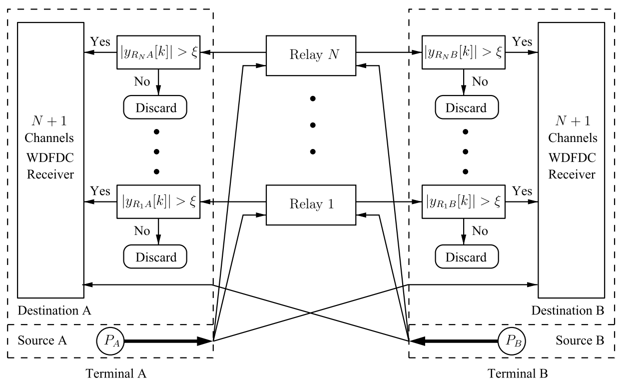

FIGURE 1. System descriptions of the multi-relay TWRN.

II. DETECT-AND-FORWARD TWO-WAY MULTIPLE RELAYING WITH WDFDC RECEIVERS

A. GENERALIZED SYSTEM MODEL

Consider a wireless network consisting of N relay nodes R_i, $i = 1, 2, \ldots, N$ and two terminal nodes A and B with direct links between them, as shown in Fig. 1. The two terminal nodes exchange information with the assistance of bidirectional relays. Differential QPSK modulation and WDFDC receivers are assumed at all nodes. In our system, a generalized TWRN model is considered using selective DetF relaying protocols. Each node has only one antenna and it works in half-duplex mode. Ideal relays are assumed in the sense that each relay knows if its decoded symbol is correct or not. The implication of this assumption and practical methods to approach such condition are considered in [28] with more details in [30]. At each destination node SNR-dependent thresholds ξ are employed to allow only the signal from the relay that transmits to be combined with the one from the source. Furthermore, all channels are assumed reciprocal as in [27], [31], and [32]. Denote the channel coefficient from node l to node j as $f_{lj}[k]$, $l, j \in \{A, B, R_i\}$. Then $f_{lj}[k], f_{jl}[k]$ are samples from the same fading process $f_{lj,jl}[\cdot]$.

TABLE 1. Different protocols of the generalized TWRN system.

Protocols	Phase 1	Phase 2	Phase 3	Phase 4	Phase 5	Relay Type
			Number of phases = 3			
P1	$A \rightarrow B,R$	$B \rightarrow A,R$	$R \rightarrow A,B$	-	-	R: Type C
			Number of phases = 4			
P2	$A \rightarrow B,R_1,R_2$	$B \rightarrow A,R_1,R_2$	$R_1 \rightarrow A,B$	$R_2 \rightarrow A,B$	-	R_1,R_2: Type C
P3	$A \rightarrow B,R_1,R_2$	$B \rightarrow A,R_1,R_2$	$R_1 \rightarrow B$	$R_2 \rightarrow A$	-	R_1,R_2: Type B
P4	$A \rightarrow B,R$	$B \rightarrow A,R$	$R \rightarrow A,B$	$R \rightarrow A,B$	-	R: Type C
P5	$A \rightarrow B,R$	$B \rightarrow A,R$	$R \rightarrow B$	$R \rightarrow A$	-	R: Type A
			Number of phases = 5			
P6	$A \rightarrow B,R_1,R_2,R_3$	$B \rightarrow A,R_1,R_2,R_3$	$R_1 \rightarrow A,B$	$R_2 \rightarrow A,B$	$R_3 \rightarrow A,B$	R_1,R_2,R_3: Type C
P7	$A \rightarrow B,R$	$B \rightarrow A,R$	$R \rightarrow A,B$	$R \rightarrow A,B$	$R \rightarrow A,B$	R: Type C

We further assume that all channels experience frequency non-selective time varying Rayleigh fading following the Jakes model [33]. Equal power allocation is assumed so that $P_A = P_B = P_{R_1} = \cdots = P_{R_N} = P/(N+2)$, where P is the total transmitted power in the system.

With the generalized TWRN model, the overall transmission is completed during at least $N+2$ phases. In the first two phases, each source broadcasts its own signal to relay nodes and the other terminal. As an example consider terminal A. During the first phase, it broadcasts the differentially encoded symbol $b_A[k]$ to relays R_i, $i = 1, 2, \ldots, N$ and terminal B. The corresponding received samples are

$$y_{AB}[k] \triangleq \sqrt{P_A} f_{AB}[k] b_A[k] + n_{AB}[k]$$

$$y_{AR_i}[k] \triangleq \sqrt{P_A} f_{AR_i}[k] b_A[k] + n_{AR_i}[k] \tag{1}$$

where $b_A[k] = a_A[k] b_A[k-1]$ and k is the index of symbol transmission time, which is the total number of phases needed to complete information exchange of two symbols, one for each direction. Then relay R_i performs WDFDC detection and decodes the symbol $\hat{a}_{AR_i}[k]$ where

$$\hat{a}_{AR_i}[k] = \arg \max_{\tilde{a}_{AR_i}[k]} \{\mathrm{Re}\{\tilde{a}_{AR_i}[k] g^*_{AR_i}[k]\}$$

$$g_{AR_i}[k] = y_{AR_i}[k] \hat{y}^*_{AR_i}[k] \tag{2}$$

and the estimated reference of the WDFDC relay receiver R_i from terminal A is [28]

$$\hat{y}_{AR_i}[k] = \sum_{\nu=1}^{L} p_{\nu_{AR_i}} \prod_{\mu=1}^{\nu-1} \hat{a}_{AR_i}[k-\mu] y_{AR_i}[k-\nu].$$

At each relay node, only a correctly decoded symbol is differentially encoded and forwarded to the destinations. Ideal relays are assumed where each relay knows if its decoded symbol is correct or not. Let $a_A[k] = e^{j\theta_A[k]}$ and $a_B[k] = e^{j\theta_B[k]}$, where $\theta_A[k]$ and $\theta_B[k]$ are phases of each information symbol. We consider three types of relays.

Type A: relay R_i serves two destinations in two phases without network coding.
1. In the first relay phase, the relay decodes the information symbol from source A. If the decoded symbol is correct, i.e. $\hat{a}_{AR_i}[k] = a_A[k]$, then $a_A[k]$ is differential encoded and transmitted to terminal B. Otherwise the relay remains silent. The encoded symbol and the received sample at destination B is

$$b_{R_iB}[k] = a_A[k] b_{R_iB}[k - m_{iB}] \tag{3}$$

$$y_{R_iB}[k] = \begin{cases} \sqrt{P_R} f_{R_iB}[k] b_{R_iB}[k] + n_{R_iB}[k], \\ \qquad \text{if } \hat{a}_A[k] = a_A[k] \\ n_{R_iB}[k], \quad \text{otherwise} \end{cases} \tag{4}$$

where $k - m_{iB}$ is the last time instant when a symbol was forwarded to terminal B.

2. In the second relay phase, the relay decodes the symbol from source B. Similarly to step 1, if the decoded symbol is correct, then $a_B[k]$ is differential encoded and transmitted to terminal A. Otherwise the relay remains silent. The encoded symbol and the received sample at destination A are

$$b_{R_iA}[k] = a_B[k] b_{R_iA}[k - m_{iA}] \tag{5}$$

$$y_{R_iA}[k] = \begin{cases} \sqrt{P_R} f_{R_iA}[k] b_{R_iA}[k] + n_{R_iA}[k], \\ \qquad \text{if } \hat{a}_B[k] = a_B[k] \\ n_{R_iA}[k], \quad \text{otherwise} \end{cases} \tag{6}$$

where $k - m_{iA}$ is the last time when a symbol was forwarded to terminal A.

Type B: the relay R_i serves only one destination in one phase without network coding.
If R_i serves destination B, it decodes the information symbol from source A and follows (3) and (4). If R_i serves destination A, it decodes the information symbol from source B and follows (5) and (6).

Type C: the relay R_i serves two destinations in one phase with network coding.
1. The relay decodes both information symbols from sources A and B.
2. If both decoded symbols are correct, i.e. $\hat{a}_{AR_i}[k] = a_A[k]$ and $\hat{a}_{BR_i}[k] = a_B[k]$, the relay performs network coding by forming a modulo-2π sum of the two symbol phases. Since the relay R_i transmits only if both decoded symbols are correct, we denote the transmission time of previously transmitted symbol as $k - m_i$ with $m_i \geq 1$, which is also the last time that the relay correctly decoded both symbols. The differentially encoded symbol at relay R_i is

$$\begin{aligned} b_{R_i}[k] &= a_{R_i}[k] b_{R_i}[k - m_i] \\ a_{R_i}[k] &= e^{j\theta_{R_i}[k]} \\ \theta_{R_i}[k] &= \theta_A[k] \oplus \theta_B[k] = (\theta_A[k] + \theta_B[k])_{2\pi}. \end{aligned} \tag{7}$$

Denote the phase of the encoded symbol $b_{R_i}[k]$ as $\varphi_{R_i}[k]$, then

$$\varphi_{R_i}[k] = \theta_{R_i}[k] \oplus \varphi_{R_i}[k - m_i]. \tag{8}$$

Then the relay broadcasts $b_{R_i}[k]$ to nodes A and B and stores $b_{R_i}[k]$ for subsequent encoding.
If either one of the decoded symbols is incorrect, the relay remains silent during its phase.
3. The sampled received signals from R_i at both terminals are

$$y_{R_iA}[k] = \begin{cases} \sqrt{P_R} f_{R_iA}[k] b_{R_i}[k] + n_{R_iA}[k], & \\ \qquad \text{if } \hat{a}_{AR_i}[k] = a_A[k] \text{ and } \hat{a}_{BR_i}[k] = a_B[k] & \\ n_{R_iA}[k], \quad \text{otherwise} & \end{cases}$$

$$y_{R_iB}[k] = \begin{cases} \sqrt{P_R} f_{R_iB}[k] b_{R_i}[k] + n_{R_iB}[k], & \\ \qquad \text{if } \hat{a}_{AR_i}[k] = a_A[k] \text{ and } \hat{a}_{BR_i}[k] = a_B[k] & \\ n_{R_iB}[k], \quad \text{otherwise} & \end{cases}$$

These relays have different capabilities. A Type A relay can serve two users in two phases where in each phase it operates similarly to an OWRN system. A type B relay can serve only one user as in OWRN. Type C relays have the capabilities of Type A relays with the addition of being able to implement network coding, and hence requiring only one phase to serve two users. While in general network coding may add delay and synchronization requirements, in our work we employ a very simple form of network coding (XOR combining) and hence these issues are not significant.

At destination nodes, SNR-dependent thresholds ξ are employed. If the magnitude of the received signal is above the threshold, the signal from the relay is combined with the one received over the direct link. First, we discuss the transmission without network coding, which corresponds to Type A and Type B relays. Take terminal A as an example. We denote the number of signal samples received at destination A from relay nodes as N_A and each signal sample is denoted by $y_{R_iA}[k]$, where $i = 1, 2, \ldots, N_A$. Assuming equal gain combining we have

$$g_A^{DF}[k] = \hat{y}_{BA}^*[k] y_{BA}[k] + \sum_{i=1}^{N_A} I_\xi[|y_{R_iA}[k]|] \hat{y}_{R_iA}^*[k] y_{R_iA}[k] \tag{9}$$

$$I_\xi[|y_{R_iA}[k]|] = \begin{cases} 1, & \text{if } |y_{R_iA}[k]| > \xi \\ 0, & \text{otherwise.} \end{cases}$$

and $\hat{y}_{BA}[k]$, $\hat{y}_{R_iA}[k]$ are the estimated references for channels BA and R_iA. With WDFDC receivers we have [28]

$$\hat{y}_{BA}[k] = \sum_{\nu=1}^{L} p_{\nu_{BA}} \prod_{\mu=1}^{\nu-1} \hat{a}_B[k-\mu] y_{BA}[k-\nu]$$

$$\hat{y}_{R_iA}[k] = \sum_{\nu=1}^{L} p_{\nu_{R_iA}} \prod_{\mu=1}^{\nu-1} \hat{a}_B[k-\mu] y_{R_iA}[k-\nu]$$

where $p_{\nu_{BA}}$ and $p_{\nu_{R_iA}}$ are the coefficients of the WDPDC receivers in the direct and relay to destination links as detailed in the next subsection. Next, we consider transmission with network coding, as performed by Type C relay. From (8), we can see that the information content in the phase of $\hat{y}_{R_iA}^*[k] y_{R_iA}[k]$ is (7). Then, in order to decode $\theta_B[k]$, terminal A needs to remove its own symbol with phase $\theta_A[k]$. Therefore, $\hat{y}_{R_iA}^*[k] y_{R_iA}[k] a_A^*[k]$ is the contribution to the combined signal and (9) becomes

$$g_A^{DF}[k] = \hat{y}_{BA}^*[k] y_{BA}[k] + \sum_{i=1}^{N_A} I_\xi[|y_{R_iA}[k]|] \hat{y}_{R_iA}^*[k] y_{R_iA}[k] a_A^*[k]$$

After signal combing, the information symbol from B is demodulated for all relay types by using

$$\hat{a}_B[k] = \arg\max_{\tilde{a}_B[k]} \{\mathrm{Re}\{\tilde{a}_B[k] (g_A^{DF}[k])^*\}\}.$$

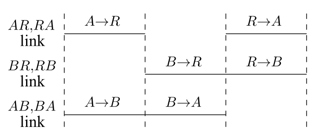

FIGURE 2. Transmission diagram of P1.

The use of different relay types results in different transmission protocols. These protocols are categorized by the number of phases that the system needs to complete a transmission round, and are summarized in Table 1. With the generalized TWRN model, the minimum number of required phases is three. This protocol, denoted as P1, has been studied in [15], [32], and [34]. As shown in Fig. 2, during the first two phases, each terminal broadcast its own symbol to the other nodes, and a Type C relay forwards the network coded

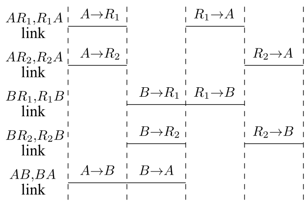

FIGURE 3. Transmission diagram of P2.

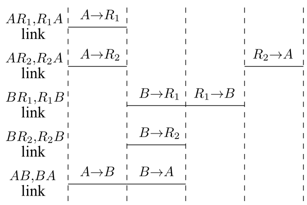

FIGURE 4. Transmission diagram of P3.

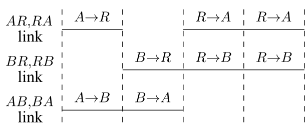

FIGURE 5. Transmission diagram of P4.

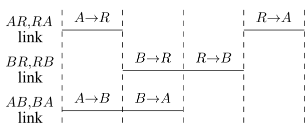

FIGURE 6. Transmission diagram of P5.

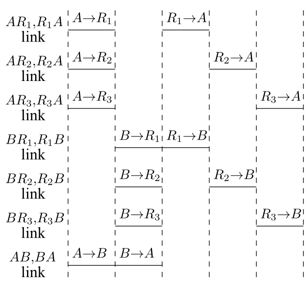

FIGURE 7. Transmission diagram of P6.

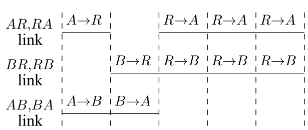

FIGURE 8. Transmission diagram of P7.

message to both destinations in the third phase. The first two phases are the same for all protocols and hence our discussion concerns only the difference between the protocols in subsequent phases. In Table 1, P1 is extended to a two Type C relays protocol which is denoted as P2. As we can see from Fig. 3, each relay in P2 consumes one phase to broadcast its network coded message to both destinations in the third and fourth phases. When the total number of phases increases to four, there are four possible protocols in Table 1. Although both P2 and P3 uses two relays, network coding is not used in P3 and each relay serves only one destination in one phase, as shown in Fig. 4. Moreover it is also possible to use one relay when the overall transmission consists of four phases. In P4, one Type C relay transmits twice using third and fourth phases when both decoded symbols are correct, as shown in Fig. 5. In P5, one Type A relay is used to forward each decoded symbol to its destination in two phases without network coding. This protocol is similar to P3, but only one relay is used in P5, as shown in Fig. 6. In fact, P5 is equivalent to OWRN in two directions and similar protocols have been studied in [15] and [34]. Furthermore, we also consider P6, where P2 is further extended to include three Type C relays. As shown in Fig. 7, each relay consumes one phase to forward network coded message to both destinations and thus five phases are needed to complete the overall transmission for P6. With the same bandwidth efficiency, P4 is also extended to allow one relay broadcasts three times to both destinations, which is denoted as P7 in Fig. 8. Comparing these seven bidirectional DetF protocols when WDFDC receivers are used is one important issue in this work.

Next, we derive an analytical method for threshold setting at destinations. Following [20], the threshold detector operation can be formulated as a binary hypothesis testing problem

$$H_1 : Y \text{ is zero mean CSCG with variance } P_R + N_0$$
$$H_0 : Y \text{ is zero mean CSCG with variance } N_0$$

where Y is a received signal sample at destination from the relay, and hypothesis H_1 corresponds to the relay being active, while H_0 to the relay being silent. Then the test $|y[k]| \underset{H_0}{\overset{H_1}{\gtrless}} \xi$ is equivalent to a likelihood ratio test, and the threshold ξ can be derived such that $(P_d - P_f)$ is maximized, where P_d is the corresponding probability of detection and P_f is the probability of false alarm. In the Appendix, we extend this approach to a general setting where multiple signal samples are observed at the destination. For P4 and P7, since the same relay transmits multiple times consecutively in one time slot, the received signal samples at destination are correlated. The decision rule is given by (68) showing that the test statistic for a relay is a quadratic form in the received signal samples and the threshold is given by (69). For other protocols, since all the samples received at the destination from different relays are independent, each WDFDC receiver compares the magnitude of its received sample to the threshold in (71) and makes a decision according to (70).

B. REGULARIZED WDFDC RECEIVERS

In [28], regularized WDFDC receivers have been considered for relay-destination channels in OWRN. It has been shown that such receiver significantly reduces the effects of feedback decision error propagation and intermittent transmissions, resulting in substantial improvement over the non-regularized WDFDC receiver. In this paper, we consider a TWRN system employing regularized WDFDC receivers over R_iA and R_iB channels, and non-regularized WDFDC receivers over AB, BA, AR_i and BR_i channels.

According to [24], for a non-regularized WDFDC receiver, the feedback coefficients p_ν,[1] $1 \leq \nu \leq L$, are obtained by minimizing the mean-square error (MSE)

$$\begin{aligned}\sigma_{mse}^2 &= E\left\{\left|y[k]-a[k]\hat{y}[k]\right|^2\right\}\\ &= E\left\{\left|c[k]-\sum_{\nu=1}^{L}p_\nu c[k-\nu]\right|^2\right\}\end{aligned} \tag{10}$$

where $c[k] \triangleq \sqrt{P}f[k]+n[k]/b[k]$. The coefficients p_ν can be obtained by solving the Yule-Walker equations

$$\Phi_c\mathbf{p}^* = \boldsymbol{\varphi_c} \tag{11}$$

where $\mathbf{p} \triangleq [p_1\ p_2\ \cdots\ p_L]^T$, $\boldsymbol{\varphi_c} \triangleq [R_c[-1]\ R_c[-2]\ \cdots\ R_c[-L]]^T$ and the autocorrelation matrix (ACM) of $c[\cdot]$ is defined as:

$$\Phi_c = \begin{bmatrix} R_c[0] & R_c[1] & \cdots & R_c[L-1] \\ R_c^*[1] & R_c[0] & \cdots & R_c[L-2] \\ \vdots & \vdots & \ddots & \vdots \\ R_c^*[L-1] & R_c^*[L-2] & \cdots & R_c[0] \end{bmatrix}$$

where $R_c[\lambda] \triangleq E\{c[k]c^*[k-\lambda]\} = PR_f[\lambda]+N_0\delta[\lambda]$. Here, $R_f[\lambda]$ is the autocorrelation function (ACF) of the fading process $f[\cdot]$, and $\delta[\cdot]$ is the discrete delta function. For Rayleigh fading following the Jake's model, we have $R_f[\lambda] = J_0(2\pi B_f T\lambda)$.

It has been shown in [28] that a mismatch exists between the calculated feedback coefficients and the actual coefficients due to decision feedback errors in the WDFDC receiver. Therefore, to reduce such mismatch, regularized receivers were proposed that include a penalty function $R = \mathbf{p}^T\mathbf{X}\mathbf{p}^*$ to the MSE of (10), resulting in the new cost criterion $C_R = \sigma_{mse}^2 + R = \sigma_{mse}^2 + \mathbf{p}^T\mathbf{X}\mathbf{p}^*$ where $\mathbf{X} = \mathrm{diag}(SNR_R^\alpha - 1, \cdots, SNR_R^\alpha - 1)$ is a $L \times L$ diagonal matrix. For TWRN, $SNR_R = (P/(N+2))/N_0$ and α is a parameter which determines the influence of SNR_R on the penalty function. Then the feedback coefficients of a regularized WDFDC receiver are obtained by solving

$$(\Phi_c + \mathbf{X})\mathbf{p}^* = \boldsymbol{\varphi_c} \tag{12}$$

When $\alpha = 0$, the penalty function is zero and (12) is equivalent to (11). In [28], based on simulation results, the parameter α is fitted to a logistic function and calculated by $\alpha_f = \frac{0.5}{1+e^{-p_2(SNR_{R,dB}-p_3)}}$ where $p_2 = 0.119878295501326$, $p_3 = 47.802208775435666$ and $SNR_{R,dB}$ is the SNR at the relay. For TWRN, $SNR_{R,dB} = 10\log_{10}((P/(N+2))/N_0)$.

[1] In this section, we omit subscripts for simplicity.

III. ANALYTICAL PERFORMANCE BOUNDS

In this section, we derive an analytical BER Ideal Lower Bound (ILB) and Ideal Tighter Lower Bound (ITLB) for different protocols of a generalized TWRN system, shown in Table 1. From the simulation results presented in section IV, we observe that for all protocols, the performance of terminal A and B is almost the same. Also, as shown in Fig. 2 to Fig. 8, for each protocol all channels experience the same Doppler frequency and the transmissions in both directions are symmetrical. Therefore, the analytical results of terminal A are the same as those for terminal B and hence only the derivation for terminal A is presented. The number of relays in the network is denoted by N and the size of the WDFDC receiver memory is denoted by L. For ILB and ITLB genie WDFDC receivers that do not include decision feedback errors are assumed. The ILB further assumes that the relay does not make detection errors and it transmits the correctly detected symbols continuously, while the ITLB assumes the relay could make detection errors. The ITLB also assumes that adjacent detection errors at the relay are spaced more than L symbols. With this assumption, the content of the memory of the WDFDC receiver at the destination will be loaded with consecutive symbols and the calculated optimum feedback coefficients p_ν can be used.

A. ILB AND ITLB FOR P3 AND P5

As shown in Table 1, both P3 and P5 consume four phases to complete a transmission cycle and no network coding is employed. The relay forwards the signal to a terminal only if it successfully detects the symbol from the other terminal. First, we consider a general case where the transmission from terminal B to A is assisted by N relays. Since the ILB assumes a relay transmits continuously, during each time slot the destination receives $N+1$ samples. A sample from the m-th channel is

$$y_m[k] = \sqrt{P_m}f_m[k]b_m[k] + n_m[k], \quad m \in \{0, 1, \ldots, N\}$$

which corresponds to $BA, R_1A, \ldots, R_NA$ channels, and the differentially encoded information symbol is given by $b_m[k] = a_B[k]b_m[k-1]$. The combined decision variable is

$$g_A^{DF}[k] = \sum_{m=0}^{N} y_m[k]\hat{y}_m^*[k]$$

where $\hat{y}_m[k]$ is the reference signal calculated by the WDFDC receiver for the m-th channel. Assuming no decision feedback errors, i.e. $\hat{a}_B[k-\mu] = a_B[k-\mu]$, then

$$\hat{y}_m[k] = \sum_{\nu=1}^{L} p_{\nu_m}\prod_{\mu=1}^{\nu-1} a_B[k-\mu]y_m[k-\nu].$$

We assume QPSK symbols $a_B[\cdot] \in \mathcal{A}_\phi = \{e^{j(\pi\nu/2+\pi/4)} | \nu \in \{0,1,2,3\}\}$ and the source transmits $a_B[k] = e^{j\pi/4}$. Then the

BER is given by [28]

$$P_b = \Pr\{\mathrm{Re}\{g_A^{DF}[k]\} < 0\} = \Pr\{D < 0\} = \int_{-\infty}^{0} p(D)dD$$
$$= -\frac{1}{2\pi j}\int_{-j\infty-\epsilon}^{j\infty-\epsilon} \frac{\phi_D(z)}{z}dz \quad (13)$$
$$D \triangleq g_A^{DF}[k] + g_A^{DF*}[k] = \sum_{m=0}^{N}(y_m[k]\hat{y}_m^*[k] + y_m^*[k]\hat{y}_m[k]) \quad (14)$$

where $\phi_D(z)$ is the characteristic function of D. In fact, D can be expressed as a Hermitian quadratic form $D \triangleq \mathbf{v}^H\mathbf{Q}\mathbf{v}$ in Circular-Symmetric Complex Gaussian (CSCG) random variables where $\mathbf{v}$ of size $2(N+1)$ and $\mathbf{Q}$ of size $2(N+1) \times 2(N+1)$ are given by

$$\mathbf{v} = \begin{bmatrix} y_0[k] & \hat{y}_0[k] & y_1[k] & \hat{y}_1[k] & \cdots & y_N[k] & \hat{y}_N[k]\end{bmatrix}^T \quad (15)$$

$$\mathbf{Q} = \mathrm{diag}(\mathbf{M}, \cdots, \mathbf{M}) \quad \text{where} \quad \mathbf{M} = \begin{bmatrix} 0 & 1 \\ 1 & 0 \end{bmatrix}. \quad (16)$$

Since $E\{f_m[k]\} = 0$ we have

$$E\{y_m[k]\} = E\{\sqrt{P_m}f_m[k]b_m[k] + n_m[k]\}$$
$$= \sqrt{P_m}E\{f_m[k]\}E\{b_m[k]\} + E\{n_m[k]\} = 0 \quad (17)$$
$$E\{\hat{y}_m[k]\} = E\{\sum_{\nu=1}^{L} p_{\nu_m}\prod_{\mu=1}^{\nu-1} a[k-\mu]y_m[k-\nu]\}$$
$$= \sum_{\nu=1}^{L} p_{\nu_m}\prod_{\mu=1}^{\nu-1} a[k-\mu]E\{y_m[k-\nu]\} = 0 \quad (18)$$

and also $E[\mathbf{v}] = \mathbf{0}$. Then the covariance matrix $\mathbf{L}$ is given by $\mathbf{L} = E\{(\mathbf{v}-\bar{\mathbf{v}})(\mathbf{v}-\bar{\mathbf{v}})^H\} = E\{\mathbf{v}\mathbf{v}^H\}$. Since the $N+1$ channels are assumed independent, we have $E\{y_m[k]y_n[k]^*\} = E\{\hat{y}_m[k]\hat{y}_n[k]^*\} = E\{y_m[k]\hat{y}_n[k]^*\} = 0$ where $m, n \in \{0, 1, \ldots, N\}$ and $m \neq n$. Hence

$$\mathbf{L} = \mathrm{diag}(\mathbf{C}_0, \cdots, \mathbf{C}_N) \quad (19)$$
$$\mathbf{C}_m \triangleq \begin{bmatrix} E\{y_m[k]y_m[k]^*\} & E\{y_m[k]\hat{y}_m[k]^*\} \\ E\{\hat{y}_m[k]y_m[k]^*\} & E\{\hat{y}_m[k]\hat{y}_m[k]^*\}\end{bmatrix}$$
$$\triangleq \begin{bmatrix} \mu_{mxx} & \mu_{mxy} \\ \mu_{mxy}^* & \mu_{myy}\end{bmatrix} \quad (20)$$

where

$$\mu_{mxx} = P_m + N_0, \quad \mu_{mxy} = e^{j\pi/4}P_m\sum_{\nu=1}^{L} p_{\nu_m}^* R_f[\nu] \quad (21)$$

$$\mu_{myy} = P_m\sum_{\nu=1}^{L}\sum_{\mu=1}^{L} p_{\nu_m}p_{\mu_m}^* R_f[\mu-\nu] + N_0\sum_{\nu=1}^{L}|p_{\nu_m}|^2 \quad (22)$$

with $P_m = P/(N+2)$ for TWRN and P denotes the total power allocated in the network.

From [35], the characteristic function of D is

$$\phi_D(z) = \prod_{n=1}^{2N+2}\frac{1}{1-z\lambda_n} \quad (23)$$

where λ_n are the eigenvalues of $\mathbf{LQ}$. From (16) and (19), we have $\mathbf{LQ} = \mathrm{diag}(\mathbf{C}_0\mathbf{M}, \cdots, \mathbf{C}_N\mathbf{M})$ showing that the eigenvalues of $\mathbf{LQ}$ are the eigenvalues of $\mathbf{C}_m\mathbf{M}$, $m \in \{0, 1, \ldots, N\}$. Denote the two eigenvalues of $\mathbf{C}_m\mathbf{M}$ by λ_{1m}, λ_{2m}. Solving $\det(\lambda\mathbf{I} - \mathbf{C}_m\mathbf{M}) = 0$, we have

$$\lambda_{1m} = \frac{1}{2}\Big[(\mu_{mxy} + \mu_{mxy}^*) - \sqrt{(\mu_{mxy} + \mu_{mxy}^*)^2 + 4(\mu_{mxx}\mu_{myy} - |\mu_{mxy}|^2)}\Big] \quad (24)$$

$$\lambda_{2m} = \frac{1}{2}\Big[(\mu_{mxy} + \mu_{mxy}^*) + \sqrt{(\mu_{mxy} + \mu_{mxy}^*)^2 + 4(\mu_{mxx}\mu_{myy} - |\mu_{mxy}|^2)}\Big] \quad (25)$$

From Cauchy–Schwarz inequality, we have $\mu_{mxx}\mu_{myy} > |\mu_{mxy}|^2$, hence $\lambda_{1m} < 0$ and $\lambda_{2m} > 0$. Based on (24) and (25), the characteristic function in (23) becomes

$$\phi_D(z) = \prod_{m=0}^{N}\frac{1}{(1-z\lambda_{1m})(1-z\lambda_{2m})} \quad (26)$$

and the BER in (13) can be expressed as

$$P_b = -\frac{1}{2\pi j}\int_{-j\infty-\epsilon}^{j\infty-\epsilon}\frac{\phi_D(z)}{z}dz$$
$$= -\frac{1}{2\pi j}\int_{-j\infty-\epsilon}^{j\infty-\epsilon}\prod_{m=0}^{N}\frac{\lambda_{1m}^{-1}\lambda_{2m}^{-1}}{z(z-\lambda_{1m}^{-1})(z-\lambda_{2m}^{-1})}dz \quad (27)$$

For a TWRN with regularized WDFDC receivers, the coefficients calculated from (12) are used for R_iA, $i \in \{1, 2, \ldots, N\}$ channels and the ones for BA channel are calculated from (11). Therefore, $\mathbf{C}_0$ and $\mathbf{C}_i$, $i > 0$ in (19) are different, resulting in $\mathbf{LQ}$ having 4 eigenvalues, $\lambda_{1B} < 0$ and $\lambda_{2B} > 0$ with order 1 and $\lambda_{1R} < 0$ and $\lambda_{2R} > 0$ with order N. Hence, (26) becomes

$$\phi_D(z) = \frac{1}{(1-z\lambda_{1S})(1-z\lambda_{2S})(1-z\lambda_{1R})^N(1-z\lambda_{2R})^N}. \quad (28)$$

and the BER in (27) becomes

$$P_b = -\frac{\lambda_{1S}^{-1}\lambda_{2S}^{-1}\lambda_{1R}^{-N}\lambda_{2R}^{-N}}{2\pi j} \times \int_{-j\infty-\epsilon}^{j\infty-\epsilon}\frac{1}{z(z-\lambda_{1S}^{-1})(z-\lambda_{2S}^{-1})(z-\lambda_{1R}^{-1})^N(z-\lambda_{2R}^{-1})^N}dz \quad (29)$$

As in [28], using contour integration, the ILB of TWRN with P3 and P5 becomes

$$\begin{aligned} P_b =& \frac{1}{(1+v_{2S1S})(1+v_{1R1S})^N(1+v_{2R1S})^N} \\ &+ \frac{1}{(1+v_{1S1R})(1+v_{2S1R})(1+v_{2R1R})^N} \\ &\times \sum_{\substack{k_2\geq 0 \\ k_2+k_3+k_4\leq N-1}} \sum_{k_3\geq 0} \sum_{k_4\geq 0} \binom{N+k_4-1}{k_4}\left(\frac{1}{1+1/v_{2R1R}}\right)^{k_4} \\ &\times \left(\frac{1}{1+1/v_{2S1R}}\right)^{k_3}\left(\frac{1}{1+1/v_{1S1R}}\right)^{k_2} \end{aligned} \tag{30}$$

with

$$v_{2S1S} \triangleq -\frac{\lambda_{2S}}{\lambda_{1S}}, \quad v_{1S1R} \triangleq -\frac{\lambda_{1S}}{\lambda_{1R}}, \quad v_{1R1S} \triangleq -\frac{\lambda_{1R}}{\lambda_{1S}},$$
$$v_{2S1R} \triangleq -\frac{\lambda_{2S}}{\lambda_{1R}}, \quad v_{2R1S} \triangleq -\frac{\lambda_{2R}}{\lambda_{1S}}, \quad v_{2R1R} \triangleq -\frac{\lambda_{2R}}{\lambda_{1R}}$$

For ITLB, since each relay only forwards the correctly decoded symbol, not all relays are active at each time instant. Hence, we denote by n_a the number of active relays. Then the BER at the destination can be expressed as

$$P_b = \sum_{n_a=0}^{N} P_{b|n_a} P_a(n_a) \tag{31}$$

where $P_a(n_a)$ is the probability that the number of active relays is n_a,

$$P_a(n_a) = \binom{N}{n_a}(1-P_{b,SR})^{n_a} P_{b,SR}^{N-n_a} \tag{32}$$

and $P_{b,SR} = 1/(1+v_{2S1S})$ is the BER of a single link non-regularized WDFDC receiver at the relay. Then (32) becomes

$$\begin{aligned} P_a(n_a) &= \binom{N}{n_a}\left(\frac{v_{2S1S}}{1+v_{2S1S}}\right)^{n_a}\frac{1}{(1+v_{2S1S})^{N-n_a}} \\ &= \frac{1}{(1+v_{2S1S})^N}\binom{N}{n_a}v_{2S1S}^{n_a}. \end{aligned} \tag{33}$$

The term $P_{b|n_a}$ in (31) is the conditional BER at the destination when the number of active relays is n_a, which is essentially (30) replacing N by n_a. Overall, from (30) and (33), (31) becomes

$$\begin{aligned} P_b =& \frac{1}{(1+v_{2S1S})^N} \\ &\times \sum_{n_a=0}^{N}\Bigg[\frac{1}{(1+v_{2S1S})(1+v_{1R1S})^{n_a}(1+v_{2R1S})^{n_a}} \\ &+ \frac{1}{(1+v_{1S1R})(1+v_{2S1R})(1+v_{2R1R})^{n_a}} \\ &\times \sum_{\substack{k_2\geq 0 \\ k_2+k_3+k_4\leq n_a-1}} \sum_{k_3\geq 0} \sum_{k_4\geq 0} \binom{n_a+k_4-1}{k_4}\left(\frac{1}{1+1/v_{2R1R}}\right)^{k_4} \\ &\times \left(\frac{1}{1+1/v_{2S1R}}\right)^{k_3}\left(\frac{1}{1+1/v_{1S1R}}\right)^{k_2}\Bigg]\binom{N}{n_a}v_{2S1S}^{n_a} \end{aligned} \tag{34}$$

For P3, the system consists of two relays and thus $P_m = P/4$ is used in (21) and (22). Compared to P3, only one relay is considered in P5 and thus we have $P_m = P/3$. For both P3 and P5, the ILB and ITLB are (30) and (34) with $N = 1$, since with P3, while having two relays, only one is used to service a terminal, and P5 employs only one relay.

B. ILB AND ITLB FOR P1, P2 AND P6

Unlike P3 and P5, all relay nodes in P1, P2 and P6 employ network coding. The network coded symbol is forwarded to both terminals only if both symbols from A and B are detected correctly. For ILB, we follow the derivation in subsection III-A and assume $a_B[k] = e^{j\pi/4}$. Then the differential encoded symbol received at terminal A can be expressed as

$$b_m[k] = \begin{cases} a_B[k]b_m[k-1], & m = 0 \\ a_C[k]b_m[k-1], & m = 1,2,\ldots,N \end{cases} \tag{35}$$

where $m \in \{0,1,\ldots,N\}$ corresponds to $BA, R_1A, \ldots, R_NA$ channels and

$$a_C[k] \triangleq a_A[k]a_B[k] \tag{36}$$

is the network coded symbol. At destination A, the signal is combined as

$$g_A^{DF}[k] = y_0[k]\hat{y}_0^*[k] + \sum_{m=1}^{N} y_m[k]\hat{y}_m^*[k]a_A^*[k] \tag{37}$$

where $y_m[k]$ and $\hat{y}_m[k]$ are

$$y_m[k] = \sqrt{P_m}f_m[k]b_m[k] + n_m[k] \tag{38}$$

$$\hat{y}_m[k] = \begin{cases} \sum_{\nu=1}^{L} p_{\nu_m}\prod_{\mu=1}^{\nu-1} a_B[k-\mu]y_m[k-\nu], \\ \qquad m = 0 \\ \sum_{\nu=1}^{L} p_{\nu_m}\prod_{\mu=1}^{\nu-1} a_C[k-\mu]y_m[k-\nu], \\ \qquad m = 1,2,\ldots,N \end{cases} \tag{39}$$

and $P_m = P/(N+2)$. Then D of (14) becomes

$$\begin{aligned} D &\triangleq g_A^{DF}[k] + g_A^{DF*}[k] \\ &= y_0[k]\hat{y}_0^*[k] + y_0^*[k]\hat{y}_0[k] \\ &\quad + \sum_{m=1}^{N}(y_m[k]\hat{y}_m^*[k]a_A^*[k] + y_m^*[k]\hat{y}_m[k]a_A[k]). \end{aligned}$$

We see that D can be expressed as the quadratic form $D \triangleq \mathbf{v}^H\mathbf{Q}\mathbf{v}$,with $\mathbf{v}$ defined as

$$\begin{aligned} \mathbf{v} = \big[&y_0[k] \quad \hat{y}_0[k] \quad y_1[k] \quad \hat{y}_1[k]a_A[k] \\ &\cdots \quad y_N[k] \quad \hat{y}_N[k]a_A[k]\big]^T \end{aligned}$$

and $\mathbf{Q}$ the same as in (16). From (17) and (18), we have $E\{y_m[k]\} = E\{\hat{y}_0[k]\} = 0$. For $m \neq 0$,

$$\begin{aligned} &E\{\hat{y}_m[k]a_A[k]\} \\ &= E\{\sum_{\nu=1}^{L} p_{\nu_m} \prod_{\mu=1}^{\nu-1} a_C[k-\mu] y_m[k-\nu] a[k]\} \\ &= \sum_{\nu=1}^{L} p_{\nu_m} E\{\prod_{\mu=1}^{\nu-1} a_C[k-\mu] a[k]\} E\{y_m[k-\nu]\} = 0 \end{aligned} \tag{40}$$

and $E[\mathbf{v}] = \mathbf{0}$. Since the $N+1$ channels are independent, the structure of the covariance matrix $\mathbf{L}$ in (19) is maintained and $\mathbf{C_0}$ is the same as in (20). However, for $m = 1, 2, \ldots, N$,

$$\begin{aligned} \mathbf{C}'_m &= \begin{bmatrix} E\{y_m[k]y_m^*[k]\} & E\{y_m[k]\hat{y}_m^*[k]a_A^*[k]\} \\ E\{\hat{y}_m[k]a_A[k]y_m^*[k]\} & E\{\hat{y}_m[k]\hat{y}_m^*[k]\} \end{bmatrix} \\ &\triangleq \begin{bmatrix} \mu_{mxx} & \mu'_{mxy} \\ \mu'^*_{mxy} & \mu_{myy} \end{bmatrix} \end{aligned} \tag{41}$$

where μ_{mxx} and μ_{myy} are the same as in (20). From (35), (36), (38) and (39), we have

$$\begin{aligned} \mu'_{mxy} &= E\{y_m[k]\hat{y}_m^*[k]a_A^*[k]\} = a_B[k]P_m \sum_{\nu=1}^{L} p_{\nu_m}^* R_f[\nu] \\ &= e^{j\pi/4} P_m \sum_{\nu=1}^{L} p_{\nu_m}^* R_f[\nu]. \end{aligned} \tag{42}$$

which is same as μ_{mxy} in (21). Therefore, for all $m \in \{0, 1, \ldots, N\}$, $\mathbf{C_m}'$ is identical to $\mathbf{C_m}$ of (20) and hence a TWRN employing network coding has the same covariance $\mathbf{L}$ as without network coding. Then eigenvalues of $\mathbf{LQ}$ are essentially (24) and (25). Thus, the ILB of TWRN with P1, P2 and P6 are (30) with $N = 1$, $N = 2$ and $N = 3$ respectively.

Next, we consider the ITLB of (31). For P1, P2 and P6, since network coding is employed, a relay transmitts only if it decodes both symbols correctly. Therefore, $P_a(n_a)$ of (32) becomes

$$P_a(n_a) = \binom{N}{n_a}((1-P_{b,SR})^2)^{n_a}(1-(1-P_{b,SR})^2)^{N-n_a} \tag{43}$$

where $P_{b,SR} = 1/(1+\nu_{2S1S})$, and then we have

$$\begin{aligned} P_a(n_a) &= \binom{N}{n_a}\left(\frac{\nu_{2S1S}}{1+\nu_{2S1S}}\right)^{2n_a}\left(\frac{1+2\nu_{2S1S}}{(1+\nu_{2S1S})^2}\right)^{N-n_a} \\ &= \frac{(1+2\nu_{2S1S})^N}{(1+\nu_{2S1S})^{2N}}\binom{N}{n_a}\frac{\nu_{2S1S}^{2n_a}}{(1+2\nu_{2S1S})^{n_a}} \end{aligned} \tag{44}$$

Since the ILB of a TWRN with P1, P2 and P6 is (30), the $P_{b|n_a}$ in (31) is (30), with N replaced by n_a. Then from (30), (31) and (44), the BER at the destination is

$$\begin{aligned} P_b &= \frac{(1+2\nu_{2S1S})^N}{(1+\nu_{2S1S})^{2N}} \sum_{n_a=0}^{N} \binom{N}{n_a}\frac{\nu_{2S1S}^{2n_a}}{(1+2\nu_{2S1S})^{n_a}} \\ &\times \Bigg[\frac{1}{(1+\nu_{2S1S})(1+\nu_{1R1S})^{n_a}(1+\nu_{2R1S})^{n_a}} \\ &+ \frac{1}{(1+\nu_{1S1R})(1+\nu_{2S1R})(1+\nu_{2R1R})^{n_a}} \\ &\times \sum_{\substack{k_2\ge 0 \\ k_2+k_3+k_4\le n_a-1}} \sum_{k_3\ge 0} \sum_{k_4\ge 0} \binom{n_a+k_4-1}{k_4}\left(\frac{1}{1+1/\nu_{2R1R}}\right)^{k_4} \\ &\times \left(\frac{1}{1+1/\nu_{2S1R}}\right)^{k_3}\left(\frac{1}{1+1/\nu_{1S1R}}\right)^{k_2}\Bigg] \end{aligned} \tag{45}$$

and the ITLB of a TWRN with P1, P2 and P6 is (45) with $N = 1$, $N = 2$ and $N = 3$ respectively.

C. ILB AND ITLB FOR P4 AND P7

As shown in Table 1, Type C relays are used with protocols P4 and P7 where network coding is employed. Compared to protocols P2 and P6 where the system consists of multiple relays and each relay transmits once over independent channels, in P4 and P7, the same relay transmits multiple times resulting in correlated samples received at the destination. We denote by N_r the number of phases that the same relay transmits consecutively. Hence we have $N_r = 2$ for P4 and $N_r = 3$ for P7. The total number of phases in one time slot is N_r+2 and the time slot is indexed by k. We index the received signal at phase i over the RD channel by $m = 1$ as $y_1[k,i]$, $i \in \{1, 2, \ldots, N_r\}$, and the corresponding estimated reference signal of WDFDC receiver is denoted as $\hat{y}_1[k,i]$. Therefore we have

$$\begin{aligned} y_1[k,i] &= \sqrt{P_1} f_1[k,i] b_1[k] + n_1[k,i] \\ \hat{y}_1[k,i] &= \sum_{\nu=1}^{L} p_\nu \prod_{\mu=1}^{\nu-1} a_C[k-\mu] y_1[k-\nu, i] \end{aligned}$$

where $P_1 = P/3$, $b_1[k]$ is given in (35) and $a_C[k]$ in (36). Also, the same coefficients p_ν, $1 \le \nu \le L$ are used for all N_r transmissions. Then the combined signal at A is

$$g_A^{DF}[k] = y_0[k]\hat{y}_0^*[k] + \sum_{i=1}^{N_r} y_1[k,i]\hat{y}_1^*[k,i]a_A^*[k]$$

where $y_0[k]$ is the received signal over channel BA of (38) and $\hat{y}_0[k]$ is the corresponding estimated reference signal of (39) with $m = 0$. Then D of (14) becomes

$$\begin{aligned} D \triangleq g_A^{DF}[k] + g_A^{DF*}[k] &= y_0[k]\hat{y}_0^*[k] + y_0^*[k]\hat{y}_0[k] \\ &+ \sum_{i=1}^{N_r}(y_1[k]\hat{y}_1^*[k,i]a_A^*[k] + y_1^*[k]\hat{y}_1[k,i]a_A[k]). \end{aligned}$$

and the corresponding $\mathbf{v}$ in the quadratic form $D \triangleq \mathbf{v}^H\mathbf{Q}\mathbf{v}$ becomes

$$\begin{aligned} \mathbf{v} = \big[&y_0[k] \quad \hat{y}_0[k] \quad y_1[k,1] \quad \hat{y}_1[k,1]a_A[k] \\ &\cdots y_1[k,N_r] \quad \hat{y}_1[k,N_r]a_A[k]\big]^T \end{aligned}$$

where $\mathbf{Q}$ is the same as in (16). From (17), (18) and (40), we have $E[\mathbf{v}] = \mathbf{0}$. Furthermore, since N_r transmissions over the *RA* channel are correlated, the covariance matrix $\mathbf{L} = E\{\mathbf{v}\mathbf{v}^H\}$ is

$$\mathbf{L} = \begin{bmatrix} \mathbf{C}_0 & 0 \\ 0 & \mathbf{C}_R \end{bmatrix},$$

$$\mathbf{C}_R = \begin{bmatrix} \mathbf{D}_{11} & \mathbf{D}_{12} & \cdots & \mathbf{D}_{1N_r} \\ \mathbf{D}_{21} & \mathbf{D}_{22} & \cdots & \mathbf{D}_{2N_r} \\ \vdots & \vdots & \ddots & \vdots \\ \mathbf{D}_{N_r1} & \mathbf{D}_{N_r2} & \cdots & \mathbf{D}_{N_rN_r} \end{bmatrix} = \begin{bmatrix} \mathbf{D}_{11} & \mathbf{D}_{21}^H & \cdots & \mathbf{D}_{N_r1}^H \\ \mathbf{D}_{21} & \mathbf{D}_{22} & \cdots & \mathbf{D}_{N_r2}^H \\ \vdots & \vdots & \ddots & \vdots \\ \mathbf{D}_{N_r1} & \mathbf{D}_{N_r2} & \cdots & \mathbf{D}_{N_rN_r} \end{bmatrix} \quad (46)$$

where the covariance $\mathbf{C}_0$ is defined in (20) with $m = 0$. The covariance matrix $\mathbf{C}_R$ corresponds to the N_r samples from the relay and $\mathbf{D}_{ij}$ is

$$\mathbf{D}_{ij} = \begin{bmatrix} E\{y_1[k,i]y_1^*[k,j]\} & E\{y_1[k,i]\hat{y}_1^*[k,j]a_A^*[k]\} \\ E\{\hat{y}_1[k,i]a_A[k]y_1^*[k,j]\} & E\{\hat{y}_1[k,i]\hat{y}_1^*[k,j]\} \end{bmatrix} \triangleq \begin{bmatrix} \mu_{1xixj} & \mu_{1xiyj} \\ \mu_{1yixj} & \mu_{1yiyj} \end{bmatrix}. \quad (47)$$

where

$$\begin{aligned} \mu_{1xixj} &= E\{y_1[k,i]y_1^*[k,j]\} = E\{(\sqrt{P_1}f_1[k,i]b_1[k] \\ &\quad + n_1[k,i])(\sqrt{P_1}f_1^*[k,j]b_1^*[k] + n_1^*[k,j])\} \\ &= P_1E\{f_1[k,i]f_1^*[k,j]\} + E\{n_1[k,i]n_1^*[k,j]\} \\ &= P_1R_f\left[\frac{i-j}{N_r+2}\right] + N_0\delta(i-j) \end{aligned} \quad (48)$$

with $R_f[\lambda] = J_0(2\pi B_f T\lambda)$. Since T is the period of one time slot and each time slot consists of $N_r + 2$ phases, the normalized Doppler frequency between two adjacent phases is $B_fT/(N_r+2)$ and the corresponding autocorrelation function is $J_0(2\pi B_fT/(N_r+2)) = R_f[1/(N_r+2)]$. In general, the number of phases between two fading samples $f[k-s,i]$ and $f[k-t,j]$ is $(t-s)\cdot(N_r+2)+(i-j)$ and therefore we have $E\{f[k-s,i]f^*[k-t,j]\} = J_0(2\pi B_fT((t-s)(N_r+2)+(i-j))/(N_r+2)) = R_f[t-s+(i-j)/(N_r+2)]$. Thus, we have

$$\mu_{1xiyj} = e^{j\pi/4}P_1\sum_{\nu=1}^{L}p_\nu^*R_f\left[\nu + \frac{i-j}{N_r+2}\right] \quad (49)$$

$$\mu_{1yixj} = e^{-j\pi/4}P_1\sum_{\nu=1}^{L}p_\nu R_f\left[-\nu + \frac{i-j}{N_r+2}\right] \quad (50)$$

$$\begin{aligned} \mu_{1yiyj} &= P_1\sum_{\nu=1}^{L}\sum_{\mu=1}^{L}p_\nu p_\mu^* R_f\left[\mu - \nu + \frac{i-j}{N_r+2}\right] \\ &\quad + \delta(i-j)N_0\sum_{\nu=1}^{L}|p_\nu|^2 \end{aligned} \quad (51)$$

We can see that when $i = j$, (48), (49) and (51) are equivalent to (21) and (22) respectively and $\mu_{1xiyj} = \mu_{1yixj}^*$. Therefore $\mathbf{D}_{ii}$ is same as $\mathbf{C_m}$ in (20) with $m = 1$ and in (46), we have $\mathbf{D}_{11} = \mathbf{D}_{22} = \cdots = \mathbf{D}_{N_rN_r} = \mathbf{C_1}$. In fact, the correlation between the multiple received samples is taken into account in $\mathbf{C}_R$ of (46). If the received N_r samples are uncorrelated, $\mathbf{C}_R$ will be diagonal and $\mathbf{L}$ of (46) will be equivalent to (19).

Since the destination A receives $N_r + 1$ signals, the characteristic function $\phi_D(z)$ is (23) where N is replaced by N_r and the ILB in (13) becomes

$$\begin{aligned} P_b &= -\frac{1}{2\pi j}\int_{-j\infty-\epsilon}^{j\infty-\epsilon}\frac{\phi_D(z)}{z}dz \\ &= -\frac{1}{2\pi j}\int_{-j\infty-\epsilon}^{j\infty-\epsilon}\frac{1}{z}\prod_{n=1}^{2N_r+2}\frac{1}{1-z\lambda_n}dz \end{aligned} \quad (52)$$

where λ_n are the eigenvalues of $\mathbf{LQ}$. From (16) and (46), we have

$$\mathbf{LQ} = \begin{bmatrix} \mathbf{C}_0\mathbf{M} & 0 \\ 0 & \mathbf{L_Q} \end{bmatrix}$$

where $\mathbf{L_Q}$ of size $2N_r \times 2N_r$ is given by

$$\mathbf{L_Q} = \begin{bmatrix} \mathbf{C}_1\mathbf{M} & \mathbf{D}_{21}^H\mathbf{M} & \cdots & \mathbf{D}_{N_r1}^H\mathbf{M} \\ \mathbf{D}_{21}\mathbf{M} & \mathbf{C}_1\mathbf{M} & \cdots & \mathbf{D}_{N_r2}^H\mathbf{M} \\ \vdots & \vdots & \ddots & \vdots \\ \mathbf{D}_{N_r1}\mathbf{M} & \mathbf{D}_{N_r2}\mathbf{M} & \cdots & \mathbf{C}_1\mathbf{M} \end{bmatrix}$$

Therefore, the eigenvalues of $\mathbf{LQ}$ are the eigenvalues of $\mathbf{C}_0\mathbf{M}$ and $\mathbf{L_Q}$. We denote the two eigenvalues of $\mathbf{C}_0\mathbf{M}$ as λ_1 and λ_2, which are (24) and (25) respectively with $m = 0$. We denote the eigenvalues of $\mathbf{L_Q}$ as $\lambda_3, \lambda_4, \ldots, \lambda_{2N_r+2}$ that are calculated numerically. For P4 and P7, we observe that each eigenvalue has order 1 and for all SNR, half of eigenvalues are on the left plane and the other half on the right plane. Therefore, for both protocols, we denote $\lambda_{2x+1} < 0$ and $\lambda_{2x+2} > 0$ where $x = 0, 1, \ldots, N_r$. Then the BER in (52) becomes

$$\begin{aligned} P_b &= -\frac{\prod_{n=1}^{2N_r+2}\lambda_n^{-1}}{2\pi j}\int_{-j\infty-\epsilon}^{j\infty-\epsilon}\frac{1}{z\prod_{n=1}^{2N_r+2}(z-\lambda_n^{-1})}dz \\ &\triangleq -\frac{\prod_{n=1}^{2N_r+2}\lambda_n^{-1}}{2\pi j}\int_{C_1}h_1(z)dz \end{aligned} \quad (53)$$

where the anticlockwise oriented contour C_1 is closed to include the left-half plane, and exclude the pole at the origin. According to the Residue Theorem [36, p. 89],

$$\int_{C_1}h_1(z)dz = 2\pi j\sum_{x=0}^{N_r}\mathrm{res}(h_1(z), z = \lambda_{2x+1}^{-1}) \quad (54)$$

where the residue at λ_{2x+1}^{-1} is given by [36, p. 90]. Since the pole λ_{2x+1}^{-1} has order 1, we have

$$\begin{aligned} &\mathrm{res}(h_1(z), z = \lambda_{2x+1}^{-1}) \\ &\quad = (z - \lambda_{2x+1}^{-1})h_1(z)|_{z=\lambda_{2x+1}^{-1}} \end{aligned}$$

$$= \frac{1}{\lambda_{2x+1}^{-1}(\lambda_{2x+1}^{-1}-\lambda_1^{-1})\cdots(\lambda_{2x+1}^{-1}-\lambda_{2x}^{-1})} \times \frac{1}{(\lambda_{2x+1}^{-1}-\lambda_{2x+2}^{-1})\cdots(\lambda_{2x+1}^{-1}-\lambda_{2N_r+2}^{-1})} \tag{55}$$

From (54) and (55), ILB in (53) becomes

$$P_b = \sum_{x=0}^{N_r} \frac{1}{(1-\frac{\lambda_1}{\lambda_{2x+1}})\cdots(1-\frac{\lambda_{2x}}{\lambda_{2x+1}})(1-\frac{\lambda_{2x+2}}{\lambda_{2x+1}})\cdots(1-\frac{\lambda_{2N_r+2}}{\lambda_{2x+1}})}. \tag{56}$$

For a TWRN with regularized receivers, λ_1 and λ_2 are calculated from (24) and (25) using the coefficients derived from (11). However, the eigenvalues of $\mathbf{L_Q}$, λ_n, $n = 3, 4, \ldots, 2N_2+2$, are calculated using regularized feedback coefficients derived from (12).

For ITLB, since the number of relay employed in the TWRN with P4 and P7 is $N = 1$, the ITLB in (31) becomes

$$P_b = P_{b|n_a=0}P_a(n_a=0) + P_{b|n_a=1}P_a(n_a=1) \tag{57}$$

where the conditional probability $P_{b|n_a=1}$ is essentially (56) and $P_{b|n_a=0}$ is derived by substituting $N_r = 0$ into (56), resulting in $P_{b|n_a=0} = 1/(1-\lambda_2/\lambda_1)$. The probability of a relay is active $P_a(n_a)$ is the same as the one for P1, which is (43) with $N = 1$. Therefore we have

$$P_a(n_a=0) = 1-(1-P_{b,SR})^2 = 2P_{b,SR} - P_{b,SR}^2$$
$$P_a(n_a=1) = (1-P_{b,SR})^2.$$

Therefore, the ITLB for P4 and P7 in (57) becomes

$$P_b = \frac{1-2\frac{\lambda_2}{\lambda_1}}{(1-\frac{\lambda_2}{\lambda_1})^3} + \frac{(\frac{\lambda_2}{\lambda_1})^2}{(1-\frac{\lambda_2}{\lambda_1})^2} \sum_{x=0}^{N_r} \frac{1}{(1-\frac{\lambda_1}{\lambda_{2x+1}})\cdots(1-\frac{\lambda_{2x}}{\lambda_{2x+1}})} \times \frac{1}{(1-\frac{\lambda_{2x+2}}{\lambda_{2x+1}})\cdots(1-\frac{\lambda_{2N_r+2}}{\lambda_{2x+1}})} \tag{58}$$

IV. SIMULATION RESULTS AND COMPARISONS

In this section, we present simulation results of a TWRN with various protocols. In all simulations, we assume WDFDC receivers with Pilot Initialization (PI), where L pilot symbols are transmitted at the beginning of the frame and the receiver starts to decode with fully loaded memory. The Hold-and-combine (HC) technique from [20] is employed for WDFDC receivers over *RD* channels where the transmission between the relay and the destination is assumed continuous. Destinations A and B, employ calculated thresholds as in the Appendix. In all simulations, Rayleigh fading with $B_fT = 0.05$ is assumed using Jake's model IV of [33], where T is the period of one time slot, i.e. the total number of phases needed to complete one transmission. We assume a frame size of $N_I = 50$ information symbols and generate at least 10^7 channel realizations. For each SNR, at least 500 bit errors are accumulated at each terminal A and B, and the results are presented as a function of SNR $= P/N_0$.

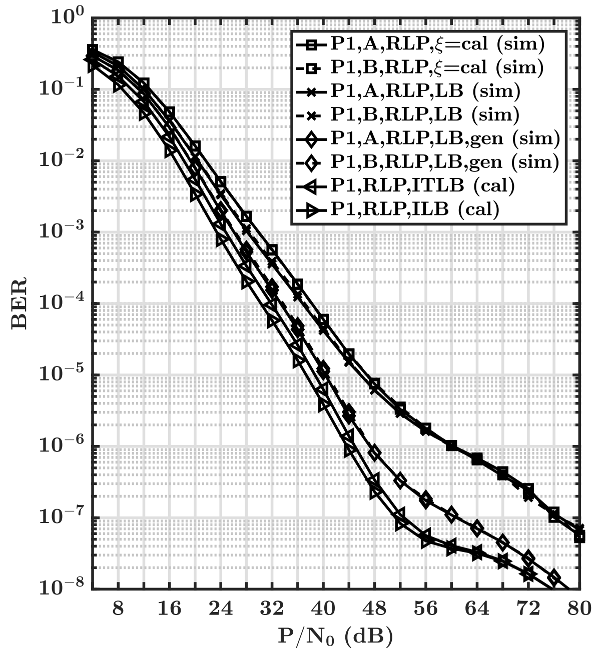

FIGURE 9. Simulated and calculated BER for a TWRN with P1, employing regularized WDFDC with fitted α_f, $N_I = 50$, $L = 4$ and $B_fT = 0.05$.

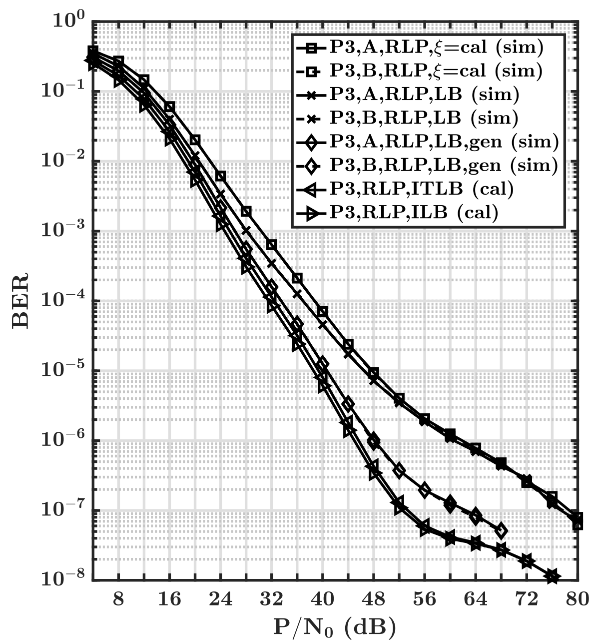

FIGURE 10. Simulated and calculated BER for a TWRN with P3, employing regularized WDFDC with fitted α_f, $N_I = 50$, $L = 4$ and $B_fT = 0.05$.

Firstly, we present a comparison of protocols P1, P3 and P5, whose simulation results are shown in Fig. 9, Fig. 10 and Fig. 11. In all figures, analytical ITLB and ILB are also plotted. For these three protocols, each terminal node receives

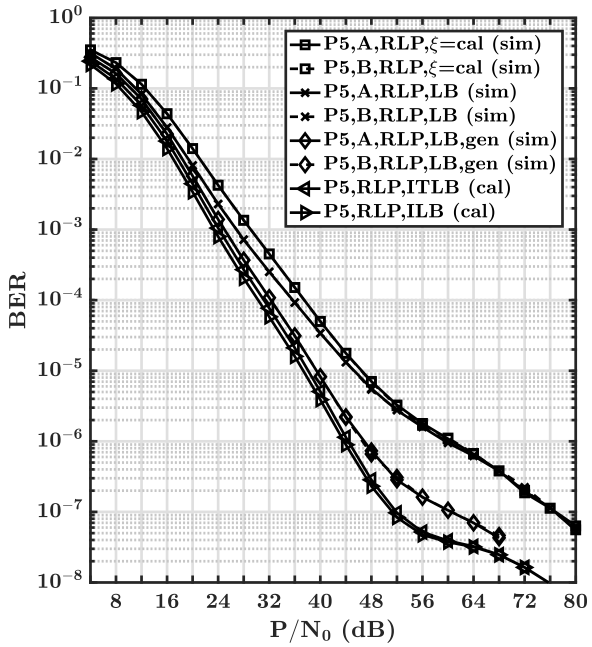

FIGURE 11. Simulated and calculated BER for a TWRN with P5, employing regularized WDFDC with fitted α_f, $N_I = 50$, $L = 4$ and $B_f T = 0.05$.

two independent signals, one from the other terminal and one from the relay. We see from these figures that the performance of these protocols is very close. Also, we observe that the performance at the two terminals is close, and hence we focus on the performance of terminal A. For P3 and P5, the relay forwards the signal to one terminal only if it correctly decodes the symbol from the other terminal, which is equivalent to OWRN in two directions. Thus, we first compare the performance of P5 and that of OWRN with $N = 1$, which is considered in [28]. Comparing Fig. 11 with [28, Fig. 12], we can see that for simulated LB and LB with genie, P5 has a performance that is parallel to OWRN when $P/N_0 < 56$ dB. This is because in P5, two terminals transmit and the power allocation follows $P_A = P_B = P_R = P/3$, while for OWRN we have $P_S = P_R = P/2$. Therefore, in theory, P5 loses $10\log_{10}(3/2) = 1.76$ dB. In Table 2, the required P/N_0 to achieve a specific BER is shown for OWRN with $N = 1$ and TWRN with different protocols. Note that the calculated ξ is not considered for OWRN in [28], and hence we do not have corresponding simulation results. We observe that at a BER of $5\cdot10^{-5}$, the performance loss of P5 over OWRN is 1.83 dB for LB, 1.78 dB for LB with genie, 1.73 dB for ITLB and 1.76 dB for ILB, which match the theoretical value. Similarly, since two relays are used in P3 and the power allocated to each node is $P/4$, the performance difference between P3 and P5 is $10\log_{10}(4/3) = 1.25$ dB. Thus, from Table 2, at the BER of $5\cdot10^{-5}$, P3 performs 1.27 dB worse than P5 for the system with calculated ξ, 1.19 dB for LB, 1.27 dB for LB with genie, 1.26 dB for ITLB and 1.24 dB for ILB.

Next, we compare P5 and P1, where both protocols employ one relay. Since in P1, symbols from A and B are network

TABLE 2. P/N_0 (dB) required to achieve BER of $5\cdot10^{-5}$ and $5\cdot10^{-7}$ for OWRN with $N = 1$ and TWRN with P1, P3 and P5 at destination A.

BER		ξ=cal	LB	LB,gen	ITLB	ILB
$5\cdot10^{-5}$	OWRN	–	36.63	32.71	31.60	30.70
	P5	40.01	38.46	34.49	33.33	32.46
	P3	41.28	39.65	35.76	34.59	33.70
	P1	40.66	39.34	35.55	34.01	32.46
$5\cdot10^{-7}$	OWRN	–	63.34	47.79	44.59	43.88
	P5	66.04	65.77	49.61	46.38	45.72
	P3	67.70	66.75	50.85	47.58	46.94
	P1	66.88	65.96	50.15	46.89	45.72

coded followed by broadcasting to both terminals at the same time, only one phase is needed for the relay to complete the transmission in both directions. Compared to P1, the relay in P5 serves one destination at a time, and hence two phases are needed. Therefore, P1 achieves higher bandwidth efficiency than P5. However, since the relay in P1 broadcasts only if both symbols are correctly decoded, the relay in P5 transmits more frequently than the one in P1 and therefore P5 provides performance advantages. As shown in Table 2, at a BER of $5\cdot10^{-5}$, the performance degradation of P1 over P5 is 0.65 dB for the system with calculated threshold, 0.88 dB for LB, 1.06 dB for LB with genie and 0.68 dB for ITLB. Note that the ILB curves for P1 and P5 are the same since in the derivation of ILB the relay is assumed to transmit continuously.

When $P/N_0 > 56$ dB, similarly to the simulation results of OWRN from [28, Fig. 12], no BER increase phenomenon is observed in Figs. 9, 10 and 11 when regularized receivers are used. It is also seen that the fitted parameters of regularized receivers derived for OWRN are applicable to TWRN as well. Furthermore, since the same regularized parameters are used, by comparing the results of LB and LB with genie in Table 2, we can see that the effects of decision feedback error propagation are almost the same for OWRN and TWRN with P1, P3 and P5 protocols. At a BER of $5\cdot10^{-5}$, the performance difference between genie simulated results (where all feedback symbols are forced to be correct), and results obtained in real operational conditions (where decision feedback symbols could suffer from errors) is 3.92 dB for OWRN, 3.97 dB for P5, 3.89 dB for P3 and 3.79 dB for P1. When P/N_0 increases and the BER is $5\cdot10^{-7}$, the difference increases to 15.55 dB for OWRN, 16.16 dB for P5, 15.9 dB for P3 and 15.81 dB for P1. This confirms our observation in [28] that the effect of decision feedback error becomes more significant at high P/N_0 also for TWRN.

We compare now protocols P1, P2 and P6, where network coding is employed in TWRN and the number of relays is $N = 1$, $N = 2$ and $N = 3$ respectively. At each relay, the network coded symbol is formed and transmitted to both terminals only if both symbols from A and B are correctly detected. For $N > 1$, transmissions of the N relays are independent. In Figs. 12 and 13 we present the performance of protocols P2 and P6. Compared to the performance for $N = 1$ in Fig. 9, we can see that as N increases, higher diversity gain is achieved. From these three figures, we see that the performance of the system with calculated ξ reaches

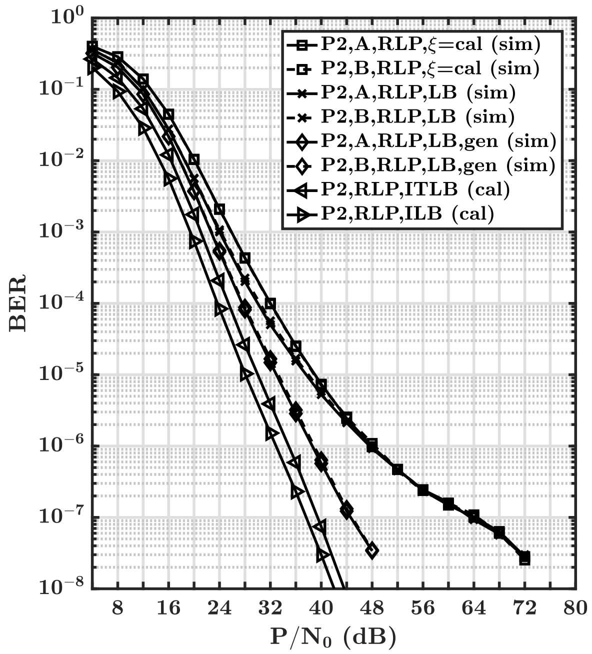

FIGURE 12. Simulated and calculated BER for a TWRN with P2, employing regularized WDFDC with fitted α_f, $N_I = 50$, $L = 4$ and $B_f T = 0.05$.

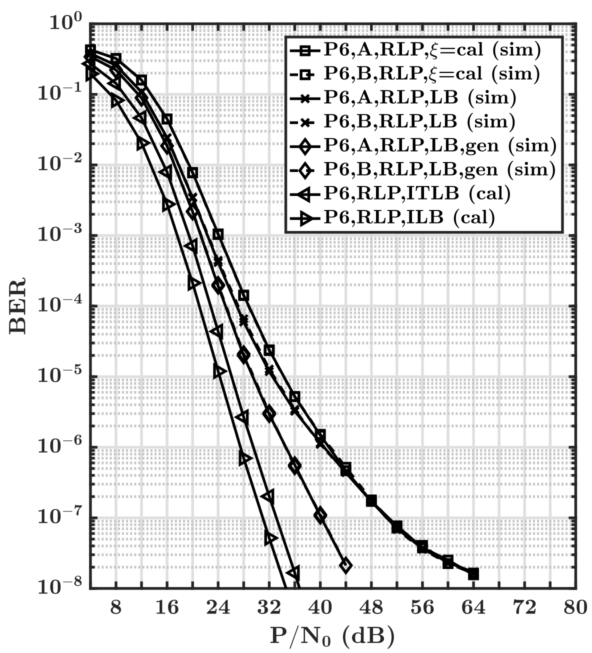

FIGURE 13. Simulated and calculated BER for a TWRN with P6, employing regularized WDFDC with fitted α_f, $N_I = 50$, $L = 4$ and $B_f T = 0.05$.

the steepest negative slope for $2 \cdot 10^{-5} \leq \text{BER} \leq 2 \cdot 10^{-1}$, which is termed as "waterfall region" in [20]. The achievable diversity order is calculated from the steepest slope estimated in this region and presented in Table 3. We see that as N increases, the achievable diversity order increases because of the increasing number of independent copies of the signal received at the destination. Compared to the achievable diversity in OWRN presented in [20, Table 2], we see that our results for TWRN match the ones for OWRN and we can conclude that TWRN achieves almost the same diversity gain as OWRN. However, since network coding is employed, relays in TWRN transmit less frequently than in OWRN. As a result, a performance loss is observed for all three protocols. Table 4 presents the SNR needed to achieve a BER of 10^{-3} when comparing the simulation results of the TWRN with calculated ξ in Figs. 9, 12 and 13 and the OWRN with SNR-dependent thresholds of Figs. 10, 14 and 15 of [20]. We see that the performance loss of TWRN decreases as N increases. In fact, the loss is due to two effects, power allocation and network coding. In TWRN, the power allocated to each node is $P/(N+2)$, while it is $P/(N+1)$ in OWRN. Therefore, the loss caused by power difference is $10\log_{10}((N+2)/(N+1))$ and the remaining performance difference results from network coding, as shown in Table 4.

TABLE 3. Diversity order based on simulation results of the system with calculated thresholds in a TWRN with regularized WDFDC receivers.

N	Achievable diversity
1 (P1)	1.21
2 (P2)	1.72
3 (P6)	2.17

TABLE 4. P/N_0 (dB) required to achieve BER of 10^{-3} for TWRN with ξ = cal in Figs. 9, 12 and 13 and OWRN with SNR-dependent ξ in Figs. 10, 14 and 15 of [20].

N	TWRN	OWRN	Perf. loss	Power loss	NetCode loss
1	29.91	26.96	2.95	$10\log_{10}(3/2) = 1.76$	1.19
2	25.89	23.6	2.29	$10\log_{10}(4/3) = 1.25$	1.04
3	24.11	22.16	1.95	$10\log_{10}(5/4) = 0.97$	0.98

Next, we consider the performance in the higher P/N_0 range. Table 5 presents the required P/N_0 to achieve BER of $5 \cdot 10^{-7}$ for TWRN with P1, P2 and P6 in Figs. 9, 12 and 13. The results for OWRN in Figs. 12, 17 and 18 of [28] are also presented. From Table 5 we can see that with calculated ξ, due to the high diversity order, P6 performs the best among the three protocols. Protocol P6 achieves 7.94 dB performance gain over P2 and 23.12 dB over P1 at a BER of $5 \cdot 10^{-7}$, which is larger than the corresponding gain of 1.78 dB and 5.80 dB at a BER of 10^{-3} from Table 4. Comparing the results of LB with LB- genie in Table 5, we see that the performance loss due to decision feedback errors is 15.81 dB for P1, 11.24 dB for P2 and 7.17 dB for P6 in TWRN. For OWRN, similar results are observed, which are 15.55 dB for $N = 1$, 11.61 dB for $N = 2$ and 7.19 dB and $N = 3$. This shows that the degradation due to decision feedback errors is similar for OWRN and TWRN. Furthermore, we see that as N increases, the effect of decision feedback errors is reduced. This is because with a larger number of relays a lower BER is achieved at the destination, and therefore the decoding errors that are fed back to the memory of WDFDC receiver are less. As explained in [28] for OWRN, also in TWRN systems the performance difference between calculated ITLB and simulated LB with genie is due to the mismatch of WDFDC coefficients caused by intermittent transmissions between relays and the destination. In Table 5, we see that the difference is 3.26 dB for P1, 4.03 dB for P2 and 5.69 dB for P6, and these are similar to the results of OWRN, which are 3.2 dB, 4.3 dB and 6.13 dB respectively. We observe that for both OWRN and TWRN, the effect of intermittent transmissions increases as N increases. This is because as N increases, more samples from relays are combined at the destination. Since each sample suffers from intermittent transmissions and they are combined with equal gain, it leads to a larger influence as N increases.

TABLE 5. P/N_0 **(dB) required to achieve BER of** $5 \cdot 10^{-7}$ **for OWRN with** $N = 1, 2, 3$ **and TWRN with P1, P2 and P6 at destination A.**

	ξ=cal		LB		LB,gen		ITLB	
N	TWRN	OWRN	TWRN	OWRN	TWRN	OWRN	TWRN	OWRN
1	66.88	–	65.96	63.34	50.15	47.79	46.89	44.59
2	51.70	–	51.58	50.09	40.34	38.48	36.31	34.18
3	43.76	–	43.45	41.99	36.28	34.80	30.59	28.67

We consider now protocols P1, P4 and P7, where all three protocols use one relay with network coding. From Table 1 we see that both protocols P2 and P4 achieve same bandwidth efficiency and use a Type C relay. As shown in Fig. 3, in the third and fourth phase of P2, each destination receives two samples from independent links. However, for P4 in Fig. 5, we see that the two received samples at each terminal are from the same link and they experience the same fading channel. Therefore, the received samples at the destination are correlated. This is the same when comparing P6 in Fig. 7 and P7 in Fig. 8. We denote N_r as the number of phases that the same relay transmits consecutively. Then we have $N_r = 1$ for P1, $N_r = 2$ for P4 and $N_r = 3$ for P7. With a selective DF protocol, the relay either keeps silent or transmits N_r times. When the relay transmits, N_r correlated samples are received from the relay at the destination, and the decision rule that compares the absolute value of one received sample to a threshold is not suitable for P4 and P7. In this case, N_r samples can be used to make a better decision regarding whether the relay transmits or not. In the Appendix, the decision rule and the corresponding threshold for P4 and P7 are derived and shown in (68) and (69).

Simulation results for protocols P4 and P7 are presented in Figs. 14 and Fig. 15. When compared to the performance of P1, we see that at low SNR, the system with calculated ξ in both figures performs worse than the one in Fig. 9. According to the decision rule of (68), the receiver at the destination either includes N_r samples from the relay in the combined detection process or does not include any. Thus, even if the threshold test passes, it is possible that some samples are only noise and are still included in the detection process. Also, it is possible that the relay transmits, but the threshold test fails and all N_r samples are discarded despite the possibility that the relay actually transmitted. Therefore, for P4 and P7, the overall performance becomes worse, especially at low SNR. We observe that at high SNR, the difference

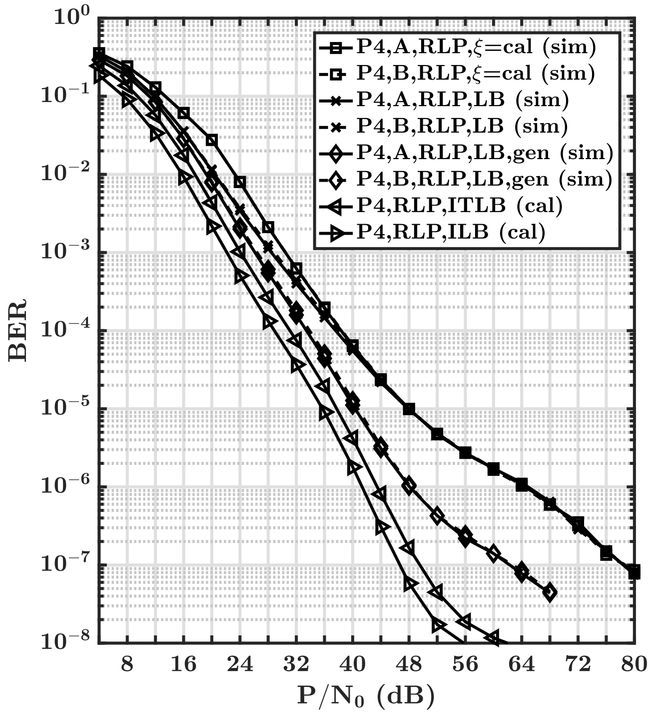

FIGURE 14. Simulated and calculated BER for a TWRN with P4, employing regularized WDFDC with fitted α_f, $N_I = 50$, $L = 4$ and $B_f T = 0.05$.

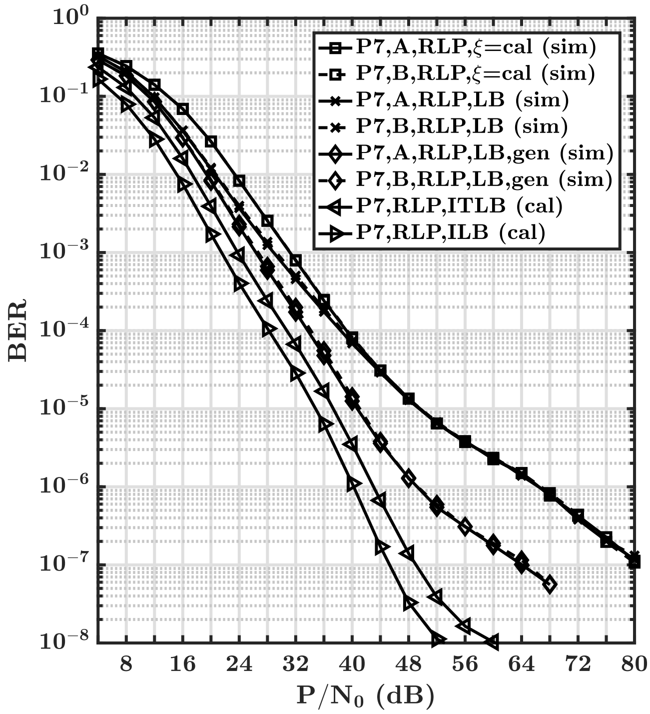

FIGURE 15. Simulated and calculated BER for a TWRN with P7, employing regularized WDFDC with fitted α_f, $N_I = 50$, $L = 4$ and $B_f T = 0.05$.

between LB with genie and ITLB increases as N_r increases in Figs. 9, 14 and 15. As shown in [28] for OWRN, this difference is due to the intermittent transmissions between the relay and the destination, which is s source of loss also in TWRN. Since each *RD* sample suffers from the mismatch of WDFDC coefficients caused by intermittent transmissions, when the samples are combined at the destination with equal gain, the intermittent transmission effect is emphasized as N_r increases.

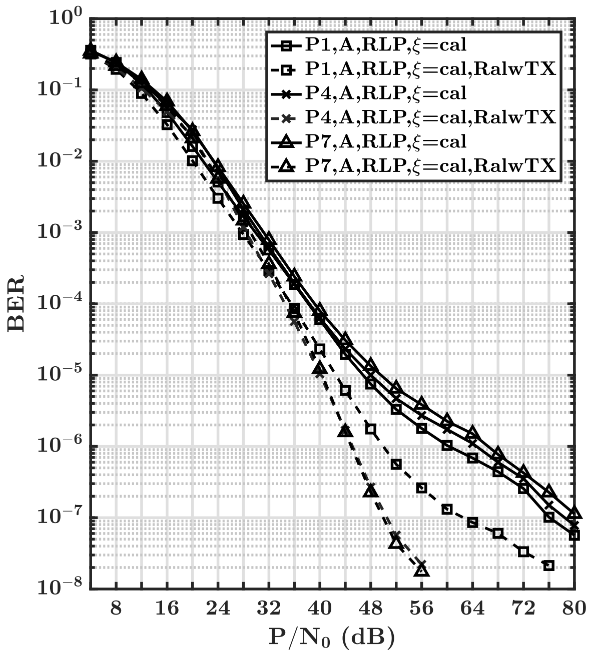

FIGURE 16. Comparison of a TWRN with P1, P4 and P7, employing regularized WDFDC with fitted α_f and calculated ξ, $N_l = 50$, $L = 4$ and $B_f T = 0.05$.

To further investigate the effect of intermittent transmissions, Fig. 16 presents simulation results of the system including the case when a relay always transmits (RalwTX). This case is compared with the results of normal operation for P1, P4 and P7. We observe that at high SNR, the performance illustrated by solid lines (normal operation) degrades as N_r increases. The dashed curves assume the relay always transmits the correct symbols, i.e. no intermittent transmissions between the relay and the destination. Under this condition, we see that at high SNR, the performance of the system improves as N_r increases. Therefore, increasing the number of correlated transmissions achieves a better performance when the relay transmits all the time. Furthermore, when we compare the paired solid and dashed curves for each protocol, we can see that the difference between them becomes larger when N_r increases. Hence we see that the effect of intermittent transmissions becomes more significant as N_r increases.

We observe that the diversity orders of P4 and P7 are similar to P1 in Fig. 16. This shows that correlated samples transmitted using protocols P4 and P7 do not provides extra diversity. Hence increasing the number of correlated transmissions from relays do not increase diversity. From Table 1, we see that both P4 and P2 involve two transmissions from the relay to the destination, and P7 and P6 both involve three. However, since the *RD* transmissions in P2 and P6 are independent, higher diversity is achieved when the number of transmission increases, as shown in Table 3.

V. CONCLUSION

This paper considers TWRN systems with regularized WDFDC receivers employing several protocols shown in Table 1. These protocols make use of three type of relays operating in DetF mode. For each protocol, we derive the optimum threshold at user terminals to detect if a relay transmits. Performance over fast fading reciprocal channels is analyzed through analytical bounds to BER, and extensive computer simulations. When protocols P3 and P5 are compared, where both are equivalent to using OWRN in two directions, we find that similar performance to OWRN is obtained. When comparing protocols P5 and P1, since P1 employs network coding reducing the number of phases required to complete a transmission cycle, we have that P1 achieves higher bandwidth efficiency than P5. However, because the relay in P1 transmits less frequently, a performance degradation over P5 is observed. Next, P2, P4, P6 and P7 are compared where all protocols use network coding, and some employ multiple transmissions from same relay. When independent signals are received at destinations from different relays, resulting in P2 and P6, then higher diversity gains are achieved as the number of relays increases. With protocols P4 and P7 multiple correlated signals are received at the destination because of multiple transmissions from same relay, resulting in no extra diversity gains. Also, a performance degradation is observed compared to P1 because of amplification of the intermittent transmission effect. In general these protocols when used with WDFDC receivers provide low error rates (without error control coding), not suffering from any error floors above a BER of 5×10^{-8}.

APPENDIX
THRESHOLD SETTING AT DESTINATIONS

In this section, we derive the optimum threshold λ for a likelihood ratio test that maximize $(P_d - P_f)$, where P_d is the probability of detection and P_f is the probability of false alarm. The observation vector is denoted by $\mathbf{Y} \triangleq [Y[1] \quad Y[2] \quad \cdots \quad Y[m]]^T$ and the binary hypothesis testing problem is formed as:

$$H_1 : \mathbf{Y} \sim p_{\mathbf{Y}|H_1}(\mathbf{y}|H_1) \tag{59}$$

$$H_0 : \mathbf{Y} \sim p_{\mathbf{Y}|H_0}(\mathbf{y}|H_0). \tag{60}$$

Then the likelihood ratio is

$$\Lambda = \frac{p_{\mathbf{Y}|H_1}(\mathbf{y}|H_1)}{p_{\mathbf{Y}|H_0}(\mathbf{y}|H_0)} \underset{H_0}{\overset{H_1}{\gtrless}} \lambda \tag{61}$$

and the corresponding P_d and P_f are

$$P_d = Pr\{\Lambda > \lambda|H_1\} \qquad P_f = Pr\{\Lambda > \lambda|H_0\}$$

The problem is to find the optimum threshold λ such that $(P_d - P_f)$ is maximized.

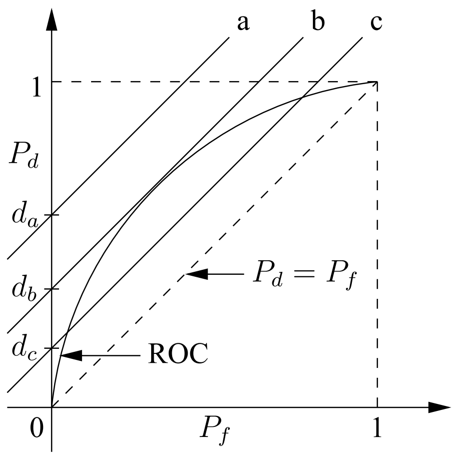

FIGURE 17. The ROC curve for the likelihood ratio test.

According to properties I and II in [37, p. 44], all continuous likelihood ratio tests have a Receiver Operating Characteristic (ROC) curve that is concave downward, above the $P_d = P_f$ line and contains the points $(P_f = 0, P_d = 0)$ and $(P_f = 1, P_d = 1)$, as shown in Fig. 17. Denote the slope of the ROC curve at $(0, 0)$ as k_{00} and the one at $(1, 1)$ as k_{11}. Then we have $k_{00} > 1$ and $k_{11} < 1$ and the slope decreases as the curve moves from $(0, 0)$ to $(1, 1)$. Consider a straight line $P_d = P_f + d$ with slope $k = 1$, then the problem of maximizing $(P_d - P_f)$ is equivalent to maximizing the value of d, which is the interception between the line and P_d axis. In Fig. 17, three lines a, b and c are presented with interceptions $d_a > d_b > d_c$. Compared to line b, line a is not achievable since there is no interception with the ROC and line c is not optimum since $d_c < d_b$. Therefore, the maximum d is achieved when the line is tangential to the ROC curve, as line b indicates. Property III of [37, p. 44] indicates that the slope of an ROC curve at a particular point is equal to the value of the threshold λ required to achieve the P_d and P_f of that point. Therefore, the optimum threshold that maximizes $(P_d - P_f)$ is the slope of line b, and we have $\lambda = 1$.

Next, we derive optimum thresholds for two special cases. In the first case, the observation vector $\mathbf{Y} = [Y_1 \quad Y_2 \quad \cdots \quad Y_m]^T$ consists of Circular-Symmetric Complex Gaussian (CSCG) random variables. In TWRN, $\mathbf{Y}$ corresponds to the received samples at the destination from the same relay in m consecutive phases. The received signal Y_i at phase i, $1 \le i \le m$, is

$$Y_i = \begin{cases} \sqrt{P_R} f_R[k,i] b_R[k] + n_R[k,i], & \text{if the relay transmits} \\ n_R[k,i], & \text{otherwise} \end{cases} \tag{62}$$

where $f_R[k,i]$, $n_R[k,i]$ are defined as the fading and noise sample of i-th phase in k-th time slot. The fading process $f_R[\cdot]$ is modelled as a correlated zero-mean CSCG random process with normalized power 1 and the noise process $n_R[\cdot]$ is an uncorrelated zero-mean CSCG random process with variance N_0. Furthermore, $f[\cdot]$ and $n[\cdot]$ are mutually uncorrelated. With the assumption of Rayleigh fading following Jake's model, the autocorrelation function is $R_f[\lambda] = J_0(2\pi B_f T \lambda)$. Hence, for transmissions at phase i and j, $1 \le i, j \le m$, in the kth time slot we have

$$\begin{aligned} E\{f_R[k,i] f_R^*[k,j]\} &= J_0(2\pi B_f T(i-j)/N_p) \\ &= R_f[(i-j)/N_p] \end{aligned}$$

where N_p is the number of phases in one time slot and $N_p = m + 2$ for TWRN with P4 and P7.

In TWRN, the hypothesis H_1 corresponds to the case when the relay transmits and the hypothesis H_0 corresponds to the case when the relay remains silent. Then (59) and (60) become

$$H_1 : \mathbf{Y} \sim p_{\mathbf{Y}|H_1}(\mathbf{y}|H_1) = \pi^{-m} det[C_1]^{-1} e^{-\mathbf{Y}^H C_1^{-1} \mathbf{Y}} \tag{63}$$

$$H_0 : \mathbf{Y} \sim p_{\mathbf{Y}|H_0}(\mathbf{y}|H_0) = \pi^{-m} det[C_0]^{-1} e^{-\mathbf{Y}^H C_0^{-1} \mathbf{Y}} \tag{64}$$

with correlation matrix C_0 specified by (65), shown at the bottom of the page, where I_m is the $m \times m$ identity matrix and

$$\begin{aligned} C_1 &= E\{\mathbf{Y}\mathbf{Y}^H | H_1\} \\ &= \begin{bmatrix} E\{Y_1 Y_1^* | H_1\} & E\{Y_1 Y_2^* | H_1\} & \cdots & E\{Y_1 Y_m^* | H_1\}\} \\ E\{Y_2 Y_1^* | H_1\} & E\{Y_2 Y_2^* | H_1\} & \cdots & E\{Y_2 Y_m^* | H_1\} \\ \vdots & \vdots & \ddots & \vdots \\ E\{Y_m Y_1^* | H_1\} & E\{Y_m Y_2^* | H_1\} & \cdots & E\{Y_m Y_m^* | H_1\} \end{bmatrix} \end{aligned}$$

where for $1 \le i, j \le m$,

$$\begin{aligned} &E\{Y_i Y_j^* | H_1\} \\ &= E\{(\sqrt{P_R} f_R[k,i] b_R[k] + n_R[k,i]) \\ &\quad \times (\sqrt{P_R} f_R^*[k,j] b_R^*[k] + n_R^*[k,j])\} \\ &= P_R E\{f_R[k,i] f_R^*[k,j]\} + \sqrt{P_R} b_R[k] E\{f_R[k,i]\} E\{n_R^*[k,j]\} \end{aligned}$$

$$\begin{aligned} C_0 = E\{\mathbf{Y}\mathbf{Y}^H | H_0\} &= \begin{bmatrix} E\{n_R[k,1] n_R^*[k,1]\} & E\{n_R[k,1] n_R^*[k,2]\} & \cdots & E\{n_R[k,1] n_R^*[k,m]\} \\ E\{n_R[k,2] n_R^*[k,1]\} & E\{n_R[k,2] n_R^*[k,2]\} & \cdots & E\{n_R[k,2] n_R^*[k,m]\} \\ \vdots & \vdots & \ddots & \vdots \\ E\{n_R[k,m] n_R^*[k,1]\} & E\{n_R[k,m] n_R^*[k,2]\} & \cdots & E\{n_R[k,m] n_R^*[k,m]\} \end{bmatrix} \\ &= N_0 I_m \end{aligned} \tag{65}$$

$$+\sqrt{P_R}b_R^*[k]E\{f_R^*[k,j]\}E\{n_R[k,i]\}+E\{n_R[k,i]n_R^*[k,j]\}$$
$$=P_R R_f[(i-j)/N_p]+N_0\delta(i-j).$$

Therefore, the covariance C_1 becomes

$$C_1=\begin{bmatrix} P_R+N_0 & P_R R_f[\frac{-1}{N_p}] & \cdots & P_R R_f[\frac{1-m}{N_p}] \\ P_R R_f[\frac{1}{N_p}] & P_R+N_0 & \cdots & P_R R_f[\frac{2-m}{N_p}] \\ \vdots & \vdots & \ddots & \vdots \\ P_R R_f[\frac{m-1}{N_p}] & P_R R_f[\frac{m-2}{N_p}] & \cdots & P_R+N_0 \end{bmatrix}$$
$$=N_0 I_m+C_\Delta=C_0+C_\Delta \tag{66}$$

where

$$C_\Delta \triangleq P_R\begin{bmatrix} 1 & R_f[\frac{-1}{N_p}] & \cdots & R_f[\frac{1-m}{N_p}] \\ R_f[\frac{1}{N_p}] & 1 & \cdots & R_f[\frac{2-m}{N_p}] \\ \vdots & \vdots & \ddots & \vdots \\ R_f[\frac{m-1}{N_p}] & R_f[\frac{m-2}{N_p}] & \cdots & 1 \end{bmatrix}. \tag{67}$$

The likelihood test in (61) can be expressed as

$$\frac{p_{\mathbf{Y}|H_1}(\mathbf{y}|H_1)}{p_{\mathbf{Y}|H_0}(\mathbf{y}|H_0)} \underset{H_0}{\overset{H_1}{\gtrless}} \lambda$$
$$\frac{\pi^{-m}det[C_1]^{-1}e^{-\mathbf{Y}^H C_1^{-1}\mathbf{Y}}}{\pi^{-m}det[C_0]^{-1}e^{-\mathbf{Y}^H C_0^{-1}\mathbf{Y}}} \underset{H_0}{\overset{H_1}{\gtrless}} \lambda$$
$$e^{\mathbf{Y}^H C_0^{-1}\mathbf{Y}-\mathbf{Y}^H C_1^{-1}\mathbf{Y}} \underset{H_0}{\overset{H_1}{\gtrless}} \lambda\frac{det[C_1]}{det[C_0]}$$
$$\mathbf{Y}^H(C_0^{-1}-C_1^{-1})\mathbf{Y} \underset{H_0}{\overset{H_1}{\gtrless}} \ln\lambda+\ln\frac{det[C_1]}{det[C_0]} \triangleq \xi. \tag{68}$$

Since $\lambda = 1$ when $(P_d - P_f)$ is maximized, the optimum threshold ξ becomes

$$\xi=\ln\frac{det[C_1]}{det[C_0]}=\ln\frac{det[C_0+C_\Delta]}{det[C_0]}$$
$$=\ln det[C_0+C_\Delta]det[C_0^{-1}]$$
$$=\ln det[(C_0+C_\Delta)C_0^{-1}]=\ln det[I_m+C_\Delta C_0^{-1}]$$
$$=\ln det\left[I_m+\frac{1}{N_0}C_\Delta\right] \tag{69}$$

In the second case, we consider $m = 1$, i.e. only one CSCG random variable Y is observed. The sampled received signal is the same as (62). From (65) and (66), we have the variances $E\{YY^*|H_1\} = P_R + N_0$ and $E\{YY^*|H_0\} = N_0$. Then the two hypothesis in (63) and (64) become

$$H_1: Y \sim p_{Y|H_1}(y|H_1)=\pi^{-1}(P_R+N_0)^{-1}e^{-\frac{|Y|^2}{P_R+N_0}}$$
$$H_0: Y \sim p_{Y|H_0}(y|H_0)=\pi^{-1}N_0^{-1}e^{-\frac{|Y|^2}{N_0}}$$

The likelihood test in (61) becomes

$$\frac{p_{Y|H_1}(y|H_1)}{p_{Y|H_0}(y|H_0)} \underset{H_0}{\overset{H_1}{\gtrless}} \lambda$$
$$\frac{\pi^{-1}(P_R+N_0)^{-1}e^{-\frac{|Y|^2}{P_R+N_0}}}{\pi^{-1}N_0^{-1}e^{-\frac{|Y|^2}{N_0}}} \underset{H_0}{\overset{H_1}{\gtrless}} \lambda$$
$$e^{(\frac{1}{N_0}-\frac{1}{P_R+N_0})|Y|^2} \underset{H_0}{\overset{H_1}{\gtrless}} \lambda\frac{P_R+N_0}{N_0}$$
$$\frac{P_R}{N_0(P_R+N_0)}|Y|^2 \underset{H_0}{\overset{H_1}{\gtrless}} \ln\lambda+\ln\frac{P_R+N_0}{N_0}$$
$$|Y|^2 \underset{H_0}{\overset{H_1}{\gtrless}} \frac{N_0(P_R+N_0)}{P_R}(\ln\lambda+\ln\frac{P_R+N_0}{N_0})$$
$$|Y| \underset{H_0}{\overset{H_1}{\gtrless}} \sqrt{\Big(N_0+\frac{N_0^2}{P_R}\Big)\Big(\ln\lambda+\ln\big(\frac{P_R}{N_0}+1\big)\Big)} \triangleq \xi. \tag{70}$$

Since $\lambda = 1$ when $(P_d - P_f)$ is maximized, then the optimum threshold in (70) becomes

$$\xi=\sqrt{\Big(N_0+\frac{N_0^2}{P_R}\Big)\ln\Big(\frac{P_R}{N_0}+1\Big)} \tag{71}$$

REFERENCES

[1] P. Mach and Z. Becvar, "Device-to-device relaying: Optimization, performance perspectives, and open challenges towards 6G networks," *IEEE Commun. Surveys Tuts.*, vol. 24, no. 3, pp. 1336–1393, 3rd Quart., 2022.
[2] P. Khuntia, R. Hazra, and P. Goswami, "A bidirectional relay-assisted underlay device-to-device communication in cellular networks: An IoT application for FinTech," *IEEE Internet Things J.*, vol. 10, no. 3, pp. 2174–2182, Feb. 2023.
[3] H. V. Nguyen, S. X. Ng, W. Liang, P. Xiao, and L. Hanzo, "A network-coding aided road-map of large-scale near-capacity cooperative communications," *IEEE Access*, vol. 6, pp. 21592–21620, 2018.
[4] N. Biswas, Z. Wang, L. Vandendorpe, and H. Mirghasemi, "On joint cooperative relaying, resource allocation, and scheduling for mobile edge computing networks," *IEEE Trans. Commun.*, vol. 70, no. 9, pp. 5882–5897, Sep. 2022.
[5] H. Pan, T.-T. Chan, V. C. M. Leung, and J. Li, "Age of information in physical-layer network coding enabled two-way relay networks," *IEEE Trans. Mobile Comput.*, vol. 22, no. 8, pp. 4485–4499, Aug. 2023.
[6] A. H. Bastami, "Two-way incremental relaying with symbol-based network coding: Performance analysis and optimal thresholds," *IEEE Trans. Commun.*, vol. 65, no. 2, pp. 564–578, Feb. 2017.
[7] S. Hatamnia, S. Vahidian, S. Aïssa, B. Champagne, and M. Ahmadian-Attari, "Network-coded two-way relaying in spectrum-sharing systems with quality-of-service requirements," *IEEE Trans. Veh. Technol.*, vol. 66, no. 2, pp. 1299–1312, Feb. 2017.
[8] F. Ono, H. Ochiai, and R. Miura, "A wireless relay network based on unmanned aircraft system with rate optimization," *IEEE Trans. Wireless Commun.*, vol. 15, no. 11, pp. 7699–7708, Nov. 2016.
[9] Y. Ye, L. Shi, X. Chu, H. Zhang, and G. Lu, "On the outage performance of SWIPT-based three-step two-way DF relay networks," *IEEE Trans. Veh. Technol.*, vol. 68, no. 3, pp. 3016–3021, Mar. 2019.
[10] Q.-Y. Yu, Y.-T. Li, W.-X. Meng, and W. Xiang, "Uniquely decodable codes for physical-layer network coding in wireless cooperative communications," *IEEE Syst. J.*, vol. 13, no. 4, pp. 3956–3967, Dec. 2019.
[11] M. Chu, R. Qiu, and X.-Q. Jiang, "Spectrum-energy efficiency tradeoff in decode-and-forward two-way multi-relay networks," *IEEE Access*, vol. 9, pp. 16825–16836, 2021.
[12] R. Vaze and R. W. Heath Jr., "On the capacity and diversity-multiplexing tradeoff of the two-way relay channel," *IEEE Trans. Inf. Theory*, vol. 57, no. 7, pp. 4219–4234, Jul. 2011.
[13] J. N. Laneman, D. N. C. Tse, and G. W. Wornell, "Cooperative diversity in wireless networks: Efficient protocols and outage behavior," *IEEE Trans. Inf. Theory*, vol. 50, no. 12, pp. 3062–3080, Dec. 2004.
[14] R. Ahlswede, N. Cai, S.-Y. R. Li, and R. W. Yeung, "Network information flow," *IEEE Trans. Inf. Theory*, vol. 46, no. 4, pp. 1204–1216, Jul. 2000.
[15] P. Popovski and H. Yomo, "Wireless network coding by amplify-and-forward for bi-directional traffic flows," *IEEE Commun. Lett.*, vol. 11, no. 1, pp. 16–18, Jan. 2007.

[16] J. Tian, Q. Zhang, and F. Yu, "Non-coherent detection for two-way AF cooperative communications in fast Rayleigh fading channels," *IEEE Trans. Commun.*, vol. 59, no. 10, pp. 2753–2762, Oct. 2011.

[17] M. Elfituri, W. Hamouda, and A. Ghrayeb, "A convolutional-based distributed coded cooperation scheme for relay channels," *IEEE Trans. Veh. Technol.*, vol. 58, no. 2, pp. 655–669, Feb. 2009.

[18] W. Su, A. K. Sadek, and K. J. R. Liu, "SER performance analysis and optimum power allocation for decode-and-forward cooperation protocol in wireless networks," in *Proc. IEEE Wireless Commun. Netw. Conf.*, Mar. 2005, pp. 984–989.

[19] T. Himsoon, W. P. Siriwongpairat, W. Su, and K. J. R. Liu, "Differential modulation with threshold-based decision combining for cooperative communications," *IEEE Trans. Signal Process.*, vol. 55, no. 7, pp. 3905–3923, Jul. 2007.

[20] G. Dai and H. Leib, "Detect-and-forward multirelay systems with decision-feedback differential coherent receivers," *IEEE Trans. Wireless Commun.*, vol. 15, no. 2, pp. 1267–1281, Feb. 2016.

[21] J. Zhang and H. Leib, "Selective decode-and-forward two-way relay network with weighted decision-feedback differential coherent detectors," in *Proc. IEEE Can. Conf. Electr. Comput. Eng. (CCECE)*, May 2016, pp. 1–5.

[22] H. Leib and S. Pasupathy, "The phase of a vector perturbed by Gaussian noise and differentially coherent receivers," *IEEE Trans. Inf. Theory*, vol. IT-34, no. 6, pp. 1491–1501, Nov. 1988.

[23] R. Schober, W. H. Gerstacker, and J. B. Huber, "Decision-feedback differential detection of MDPSK for flat Rayleigh fading channels," *IEEE Trans. Commun.*, vol. 47, no. 7, pp. 1025–1035, Jul. 1999.

[24] R. Schober and W. H. Gerstacker, "Decision-feedback differential detection based on linear prediction for MDPSK signals transmitted over Ricean fading channels," *IEEE J. Sel. Areas Commun.*, vol. 18, no. 3, pp. 391–402, Mar. 2000.

[25] C. Xu, S. X. Ng, and L. Hanzo, "Multiple-symbol differential sphere detection and decision-feedback differential detection conceived for differential QAM," *IEEE Trans. Veh. Technol.*, vol. 65, no. 10, pp. 8345–8360, Oct. 2016.

[26] C. Stierstorfer, R. F. H. Fischer, and G. Yammine, "Iterative decision-feedback in non-coherent multi-user massive MIMO systems," in *Proc. 19th Int. ITG Workshop Smart Antennas*, Mar. 2015, pp. 1–8.

[27] T. Cui, F. Gao, and C. Tellambura, "Differential modulation for two-way wireless communications: A perspective of differential network coding at the physical layer," *IEEE Trans. Commun.*, vol. 57, no. 10, pp. 2977–2987, Oct. 2009.

[28] J. Zhang and H. Leib, "Regularized WDFDC receivers for selective detect-and-forward multi-relaying systems," *IEEE Open J. Veh. Technol.*, vol. 1, pp. 130–145, 2020.

[29] J. Proakis and M. Salehi, *Digital Communications*, 5th ed. New York, NY, USA: McGraw-Hill, 2008.

[30] J. Zhang, "Selective decode-and-forward bidirectional multi-relay networks with regularized weighted decison feedback differential coherent receivers," M.S. thesis, Dept. Elect. Comput. Eng., McGill Univ., Montreal, QC, Canada, Jul. 2017.

[31] B. Rankov and A. Wittneben, "Spectral efficient protocols for half-duplex fading relay channels," *IEEE J. Sel. Areas Commun.*, vol. 25, no. 2, pp. 379–389, Feb. 2007.

[32] T. Cui, F. Gao, T. Ho, and A. Nallanathan, "Distributed space-time coding for two-way wireless relay networks," *IEEE Trans. Signal Process.*, vol. 57, no. 2, pp. 658–671, Feb. 2009.

[33] A. Alimohammad, S. F. Fard, B. F. Cockburn, and C. Schlegel, "An accurate and compact Rayleigh and Rician fading channel simulator," in *Proc. IEEE Veh. Technol. Conf.*, May 2008, pp. 409–413.

[34] S. J. Kim, N. Devroye, and V. Tarokh, "Bi-directional half-duplex relaying protocols," *J. Commun. Netw.*, vol. 11, no. 5, pp. 433–444, Oct. 2009.

[35] G. L. Turin, "The characteristic function of Hermitian quadratic forms in complex normal variables," *Biometrika*, vol. 47, no. 1/2, pp. 199–201, Jun. 1960.

[36] M. Evgrafov, *Analytic Functions* (Saunders Mathematics Books). Philadelphia, PA, USA: Saunders, 1966.

[37] H. Van Trees, *Detection, Estimation, and Modulation Theory, Part I*. Hoboken, NJ, USA: Wiley, 2001.

JUNQIAN ZHANG was born in Taiyuan, Shanxi, China, in 1989. He received the B.A.Sc. degree in electrical engineering from the University of Toronto, Toronto, ON, Canada, in 2014, and the M.Eng. degree in electrical engineering from McGill University, Montreal, QC, Canada, in 2017. From 2014 to 2017, he was a Research Assistant with McGill University. He is currently a Digital Design Engineer with the Communication Infrastructure Team, Analog Devices Inc., working on digital system design for communication systems. His research interests include cooperative communication, relay networks, differential modulation systems, WDFDC receivers, and modeling of communication systems.

HARRY LEIB (Life Senior Member, IEEE) received the B.Sc. (cum laude) and M.Sc. degrees in electrical engineering from the Technion—Israel Institute of Technology, Israel, in 1977 and 1984, respectively, and the Ph.D. degree in electrical engineering from the University of Toronto, Canada, in 1987. After completing the Ph.D. degree, he was a Postdoctoral Research Associate and an Assistant Professor with the University of Toronto. Since September 1989, he has been with the Department of Electrical and Computer Engineering, McGill University, where he is currently a Full Professor. His current research interests include digital communications, wireless communication systems, global navigation satellite systems, detection, estimation, and information theory. He was an Editor of the IEEE Transactions on Communications, from 2000 to 2013, an Associate Editor of the IEEE Transactions on Vehicular Technology, from 2001 to 2007, and a Guest Co-Editor for Special Issues of the IEEE Journal on Selected Areas in Communication on "Differential and Noncoherent Wireless Communication," from 2003 to 2005, and "Spectrum and Energy Efficient Design of Wireless Communication Networks," from 2012 to 2013. Since 2017, he has been the founding Editor-in-Chief of *AIMS Electronics and Electrical Engineering* journal.